Astrophysical Instabilities:
the formation and pulsation of stars

Mike Montgomery (IoA, Cambridge)

February 12, 2004

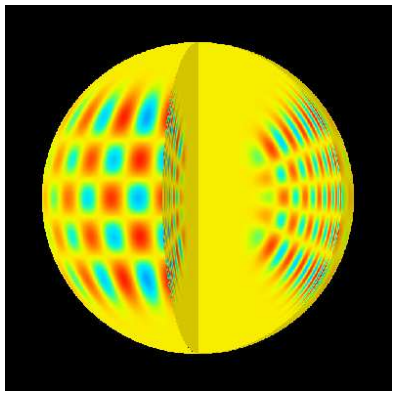

Outline
(subject to revision)

Part I: Star Formation

1. Introduction: physical processes
2. Molecular Clouds
3. Gravitational Collapse and the Formation of Single Stars
4. Discs, Accretion, and Outflows
5. Pre-main-sequence Stellar Evolution

Part II: Stellar Pulsations

1. Introduction and Basic Theory
2. Eigenmodes, Driving of Pulsations
3. Time Series Observations: aliasing
4. Seismology:
   a. solar inversions ('helioseismology')
   b. fits for other stars ('asteroseismology')

Star Formation

Why is understanding stars important?

- stars contain most of the luminous mass in the universe
- stars are the 'fundamental' building blocks of open clusters, globular clusters, and galaxies, analogous to the way that atoms are the building blocks of matter
- unlike atoms, individual stars evolve, having a beginning and an end, and they have a continuous spectrum of characteristics (in mass, luminosity, etc.)

Star formation itself is intimately related to other fields in astronomy:

- the interstellar medium (ISM)
- chemical abundances and evolution
- galaxy evolution
- stellar populations (incidence of binarity, distribution of masses, pop I & II (& III ?) stars)
- stellar systems (open clusters, globular clusters, cataclysmic variables)
- planetary systems

Intrinsically, of course, the phenomenon of star formation is interesting in and of itself, involving many different physical processes:

- Gravity
- Magneto-hydrodynamics (MHD)
- Radiative transfer
- Chemical processes
- Accretion disks
- Jets

So what kinds of questions would we like to be able to answer?

- when and where do stars form?
- what is the efficiency?
- what is the distribution of masses? (the 'initial mass function' — IMF), and is it universal?
- Do most stars form in clusters or in isolation?
- How are binaries formed?
- How does metallicity affect star formation?
  – difference between pop II and primordial star formation?
- Does collapse proceed from a quasi-equilibrium state, or is the cloud in a state of turbulence?

- Role of Rotation?
- Role of Magnetic fields?
- How do discs form and operate?
- How do jets/bipolar outflows operate?
- How do planets form?

Well, these are the things one would eventually like to know about, but we are not very close to understanding many of these points, whereas other points are fairly well-understood from an observational perspective.

Recent Star Formation: Young Stars

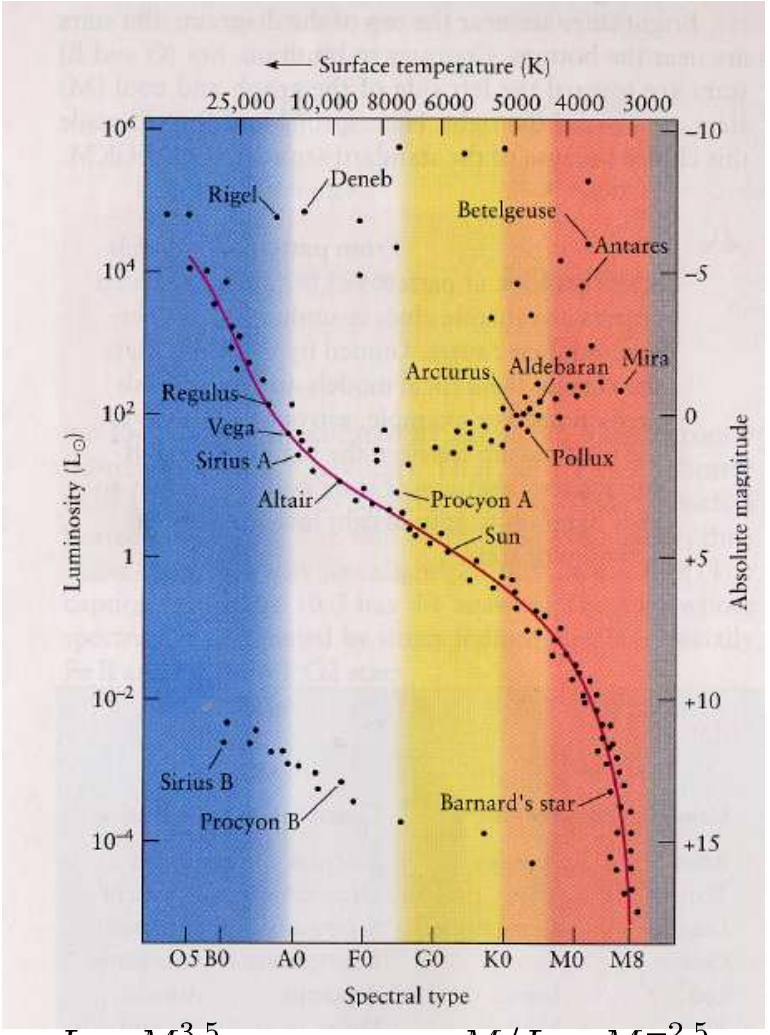

$$L \propto M^{3.5} \quad \Rightarrow \quad \tau_{\rm MS} \propto M/L \propto M^{-2.5}$$

Massive stars have *much* shorter MS lifetimes than the Sun, of order 10^6 years.

Evidence of recently formed stars

- For massive stars
  - — young if still on main sequence
  - — not visible before main sequence
- For low-mass stars
  - – visible before main sequence: T-Tauri stars (variable, have emission lines)
  - – more rapidly rotating and more convective than their main sequence counterparts
    $\Rightarrow$ more magnetic activity
  - – show infrared *and* UV excess attributable to an accretion disk

Observational estimates of collapse timescales

From the observed relative numbers of systems in different stages of collapse, the following timescales have been inferred:

Phase	Time
Pre-collapse molecular cloud	up to 10^7 years
Collapse	$\sim 10^5$ years
Post-collapse/pre-main sequence	$\sim 10^7$ years

The Virial Theorem

Say you've got a self-gravitating fluid (Spitzer, pp. 215–17; Shu, pp. 328–337):

$$\rho\frac{D\vec{v}}{Dt} = -\nabla p - \rho\nabla\Phi - \frac{1}{8\pi}\nabla B^2 + \frac{1}{4\pi}\vec{B}\cdot\nabla\vec{B}$$

Now take the scalar product of $\vec{r}$ with this equation and integrate over the volume interior to a chosen co-moving surface. After an integration by parts, we have

$$\frac{1}{2}\frac{D^2 I}{Dt^2} = 2E_{\rm kin} + 3\Pi + E_{\rm mag} + E_{\rm grav} \equiv \nu$$

where

$$\begin{aligned}
I &\equiv \int \rho r^2 dV \quad \text{(moment of inertia)} \\
E_{\rm kin} &\equiv \tfrac{1}{2}\int \rho v^2 dV \quad \text{(non-thermal kinetic energy)} \\
\Pi &\equiv \int p dV \quad (\sim \text{thermal energy}) \\
E_{\rm mag} &\equiv \tfrac{1}{8\pi}\int B^2 dV \quad \text{(magnetic energy)} \\
E_{\rm grav} &\equiv \tfrac{1}{2}\int \rho\Phi dV \quad \text{(gravitational energy)}
\end{aligned}$$

In order for collapse to occur, gravity must dominate all other sources of support, i.e.,

$$-E_{\rm G} > 3\Pi + E_{\rm mag} + 2E_{\rm kin} + \ldots$$

Jeans Mass

Assuming a spherical, uniform density, isothermal cloud, and an ideal gas equation of state, $P = nk_BT = \rho R_g T/\mu$, and considering only thermal support, we find

$$\frac{3}{5}\frac{GM^2}{R} > \frac{3MR_gT}{\mu}$$

$$\Rightarrow M_{\rm J} = \left(\frac{5R_gT}{G\mu}\right)^{3/2}\left(\frac{3}{4\pi\rho}\right)^{1/2} \quad \text{(Jeans Mass)}$$

or $$R_{\rm J} = \left(\frac{15}{4\pi}\frac{R_gT}{\mu G\rho}\right)^{1/2} \quad \text{(Jeans radius)}$$

- Clouds with $M > M_{\rm J}$ ($R > R_{\rm J}$) will collapse.
- Can be derived from a more formal stability analysis ("the Jeans Swindle").

Can thermodynamics halt the collapse?

Consider contraction with the following polytropic relation:

$$P \propto \rho^{\gamma} \quad \Rightarrow \quad T \propto \rho^{\gamma-1}$$

so

$$\begin{aligned} \nu &\approx -a\frac{M^2}{R} + bMT \\ &= -a\frac{M^2}{R} + bM\left(\frac{M}{R^3}\right)^{\gamma-1} \\ &= -a\frac{M^2}{R}\left(1 - \frac{b}{a}M^{\gamma-2}R^{4-3\gamma}\right) \end{aligned}$$

If $\gamma > 4/3$, then ν will become zero as R decreases, so collapse can be halted

If $\gamma < 4/3$, then ν remains negative, so collapse proceeds

What about rotation?

For rotation,

$$E_{\rm kin} = \frac{1}{2}I\Omega^2 \sim MR^2\Omega^2$$

Due to conservation of angular momentum

$$L = I\Omega \sim MR^2\Omega = \text{const.},$$

so

$$\begin{aligned} \nu &\approx -a\frac{M^2}{R} + bMR^2\Omega^2 \\ &= -a\frac{M^2}{R} + b\frac{L^2}{MR^2} \\ &= -a\frac{M^2}{R}\left(1 - \frac{bL^2}{aM^3R}\right) \end{aligned}$$

Thus, as R decreases there will always come a point at which $\nu = 0$, and the collapse is halted.

Magnetic Fields?

$$E_{\rm mag} \sim B^2 V \sim B^2 R^3$$

If the flux is frozen to the fluid, then the flux across any surface is constant, so

$$\Phi_m \sim BR^2 = \text{const.},$$

so

$$\begin{aligned} \nu &= -a\frac{M^2}{R} + bB^2R^3 \\ &= -a\frac{M^2}{R} + b\frac{\Phi_m^2}{R} \\ &= -a\frac{M^2}{R}\left(1 - \frac{b\Phi_m^2}{aM^2}\right) \end{aligned}$$

$\Rightarrow$ Magnetic field cannot halt collapse

But we can define a "magnetic Jeans mass" for gravity to overcome magnetic pressure:

$$-E_{\rm G} > E_{\rm mag} \quad \Rightarrow \quad M_J = \frac{BR^2}{(3.6G)^{1/2}}$$

Typical values

for the (usual) thermal Jeans mass, M_J(therm), and the magnetic Jeans mass, M_J(mag):

	n (cm^{-3})	B (G)	T (K)	M_J(therm) ($M_\odot$)	M_J(mag) ($M_\odot$)
Interstellar gas	10	10^{-6}	100	10^4	10^4
GMC's	10^2–10^3	3×10^{-5}	10	10	10^3
Dense cores	10^4	10^{-5}	10	$\gtrsim 1$	$\gtrsim 1$

Angular Momentum

Specific angular momentum of GMC's is much greater than that of the stars which they form:

Object	$J(L/M)$
molecular cloud ~ 1 pc	$> 10^{23}$
dense cloud core ~ 0.1 pc	10^{21}
Sun	10^{15}
3-day to 10^4-year binary	10^{19}–10^{21}
T-Tauri star	10^{17}
Discs/Jupiter	10^{20}

$\Rightarrow J_{GMC} \gtrsim 10^6 J_\odot$

Specific angular momentum must be transported away from star forming regions

— Pre-collapse: Magnetic braking:
tries to enforce uniform rotation on a cloud, transports angular momentum outward

— Collapse: Formation of binaries/discs

— Accretion phase: viscous processes in accretion disc transport angular momentum outward and mass inward

— Stars:
magnetic breaking through stellar winds

Heating and Cooling in Clouds

- Cooling
  - — At low densities and high temperatures ($T \sim$ 100–1000 K), molecules radiate, e.g., H_2, CO
  - — At high densities and moderate temperatures ($T \gtrsim 15$ K) dust grains radiate
- Heating
  - – External radiation: X-ray, UV, and other radiation
  - – Cosmic rays

(Hayashi, C. 1966, ARA&A, 4, 171)

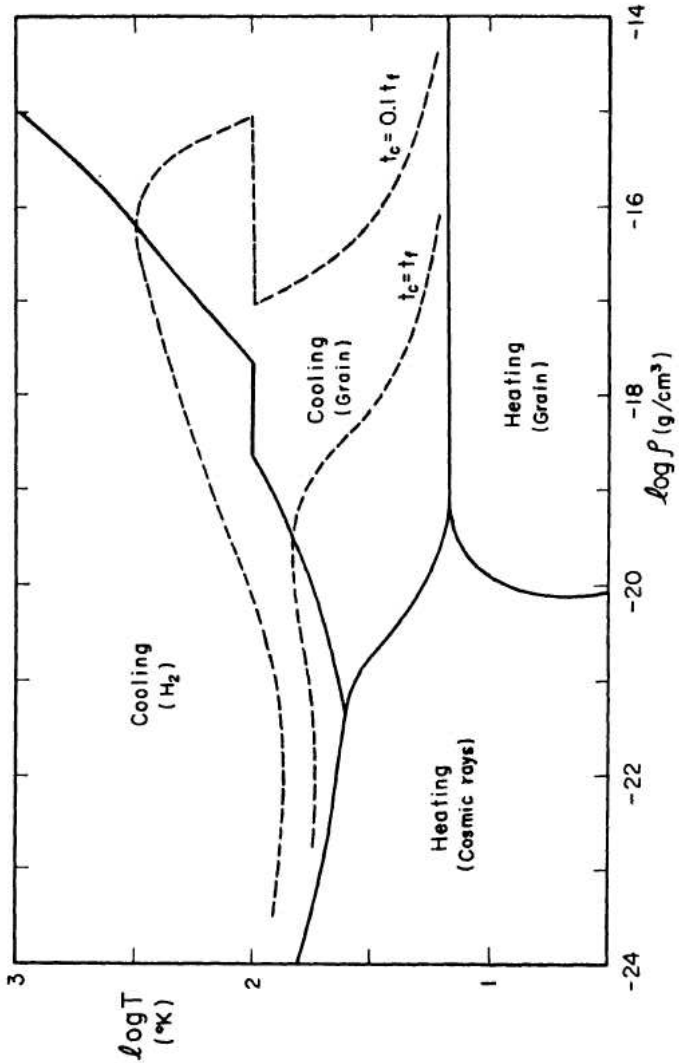

FIG. 2. The comparison of the cooling and heating processes for completely transparent stars. The solid curves represent the boundaries of the regions where each of the four processes is predominant.

Ambipolar diffusion

- The drift of neutral atoms/molecules relative to ions which are tied to a magnetic field

— this drift is produced by the competing forces of gravity, which acts on both the ions and neutrals, and the magnetic field, which acts only on the ions

- timescale (Spitzer, pp 294–295)

$$\frac{GM\rho}{R^2} = n_i \langle v_{\rm th}\sigma_{\rm coll}\rangle n_{\rm H_2} m_{\rm H_2} u_D$$

$$u_D = \frac{4\pi}{3}\frac{GRm_{\rm H_2}}{\langle v_{\rm th}\sigma_{\rm coll}\rangle}\frac{n_{\rm H_2}}{n_i}$$

$$t_{\rm ambi} = \frac{R}{u_D} = \frac{3}{4\pi}\frac{\langle v_{\rm th}\sigma_{\rm coll}\rangle}{Gm_{\rm H_2}}\frac{n_i}{n_{\rm H_2}}$$

$$= 5.0\times 10^{13}\frac{n_i}{n_{\rm H_2}} \text{ years}$$

In high density regions the ionization fraction can get as low as

$$\frac{n_i}{n_{\rm H_2}} \gtrsim 10^{-7},$$

$$\Rightarrow t_{\rm ambi} \gtrsim 5\times 10^6 \text{ years}$$

– long enough for cloud lifetime ($\sim 10^7$ years)

– too long for initial star formation:

$\lesssim 10\%$ of GMC's do not have stars

Time until first star formation is

$\sim 0.1 t_{\rm GMC} \sim 10^6$ years $\ll t_{\rm ambi}$

– more importantly, M_J(mag)$\sim 10^3 M_\odot$ for average GMC conditions

– cannot form cores with $M \sim$ a few $M_\odot$

Turbulence

Turbulence, through its kinetic energy, also offers a mechanism for support in GMC's. In the case of fully developed, homogeneous, isotropic turbulence, the kinetic energy spectrum is the given by the "Kolmogorov" scaling law:

$$E_{\rm total} = \int_{k_0}^{\infty} dk E_k, \qquad E_k \propto k^{-5/3}$$

The fact that such turbulence has a power law dependence on length scales (k) means that it is self-similar over this range. As we will see, GMC's also exhibit self-similar behaviour, which has led many to seek an explanation for this in terms of the turbulence of the cloud.

Since there is no general theory of turbulence, and consequently no simple scaling relation for how it would evolve during collapse, we have not attempted to estimate its effects in any semi-quantitative way.

- decay of turbulence may be important for onset of collapse
- magnetic fields may be important for sustaining turbulence

References for the virial theorem, ambipolar diffusion, and turbulence

"Gas Dynamics", vol. II, Frank Shu, 1992

"Physical Processes in the Interstellar Medium", Lyman Spitzer, 1978

Also, the "special edition" issue on star formation in *Science* is a good general reference:

http://www.sciencemag.org/content/vol295/issue5552/#specialintro

Molecular Clouds:

sites of star formation

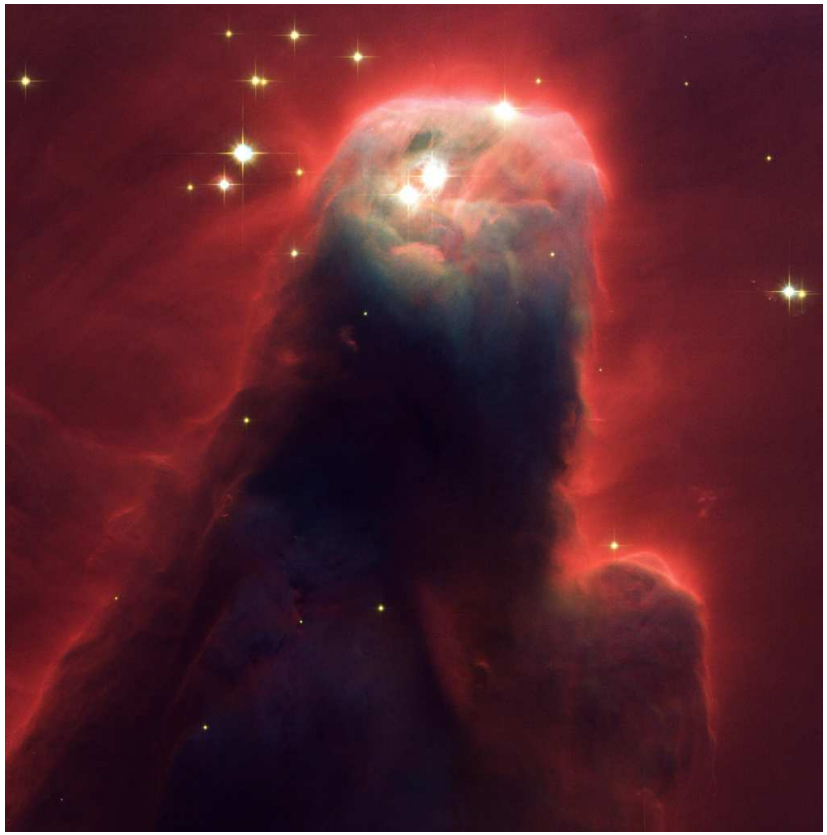

The Cone Nebula (NGC 2264)

The Omega Nebula (aka, M17 and "The Swan Nebula")

Molecular Cloud Structure

Giant molecular clouds are composed of complexes of individual molecular clouds

definitions

molecular clouds: regions of the ISM in which the gas is primarily molecular

- detected in CO millimeter emission
- GMC's (giant molecular clouds) have masses $\gtrsim 10^4 M_\odot$, but small clouds may have $\gtrsim 10^2 M_\odot$

clumps: regions of high-pressure and density in GMC's

- the sites of clustered star formation
- may comprise a small fraction of the total volume of the complex ($\sim 3\%$)

cores: regions out of which single stars (or multiple systems such as binaries) form

Structure of Molecular Clouds

- non-uniform
- GMC's in the Milky Way have mass ranges of 10^5 to $10^{6.5} M_\odot$
- spatial scales of 10–100 pc
- median radius of ~ 20 pc, median mass of $3.3 \times 10^5 M_\odot$
- have a power law mass spectrum of

$$\frac{dN_{\rm GMC}}{dM_{\rm GMC}} \propto M_{\rm GMC}^{-1.6}$$

mass between M_1 and M_2 ($M_2 > M_1$) is

$$\begin{aligned} M_{\rm total} &\sim \int_{M_1}^{M_2} dM\, M \frac{dN}{dM} \\ &\propto M_2^{0.4} - M_1^{0.4} \end{aligned}$$

$\Rightarrow$ more mass is contained in the larger clouds than the smaller clouds

The Antennae

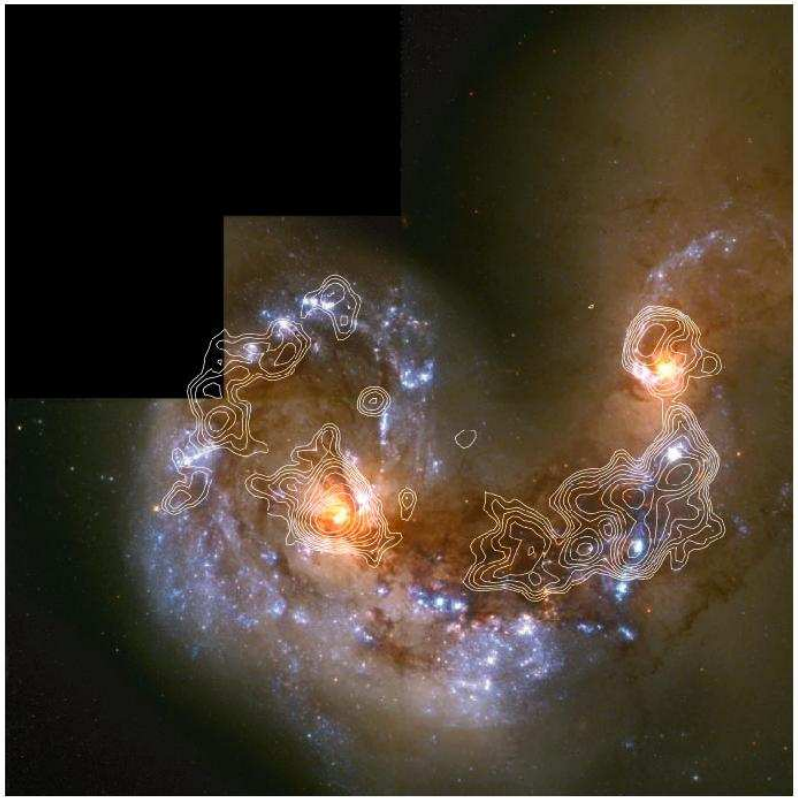

Fig. 2. A CO integrated intensity map (white contours) overlaid on a true color HST image of the Antennae galaxies (*95*) from (*21*). [Courtesy Christine Wilson] The young SSCs are the bright blue objects seen in this image.

$$\frac{dN_{\rm GMC}}{dM_{\rm GMC}} \propto M_{\rm GMC}^{-1.4\pm0.1}$$

Aside:

- The Main difference between starbursting systems and the GMC's in the Milky Way is the upper mass limit for the GMC's (larger in starbursting systems); otherwise, they appear to be the same
- The observations seem to suggest that the SGMC's ("supergiant molecular clouds") in the Antennae were formed by the agglomeration of smaller clouds (e.g., GMC's)
- It may be that *all* GMC's and SGMC's are produced from the agglomeration of smaller clouds
- Since the physics of agglomeration does not depend on local quantities, we would expect there to be a universal mass function for GMC's if they are formed by agglomeration

Back to molecular cloud structure...

- measured linewidths are dominated by turbulent motions
  $\Delta v_{\rm turb} \sim 0.2 - 15$ km/s $c_s \sim 0.15$ km/s,
  $\Rightarrow \Delta v_{\rm turb} \gg c_s$
- Clouds display self-similar/fractal structure over a large range of length scale

  Larson scaling relations:
  - *Mean* density versus size:
    $\rho \propto R^{\alpha}$, $\alpha \sim -1.15 \pm 0.15$
    $\Rightarrow M \propto R^{1.85}$ (a volume filling factor of 1 would give $M \propto R^3$)
  - Velocity dispersion, Δv, versus size:
    $\Delta v \propto R^{\beta}$, $\beta \sim 0.4 \pm 0.1$

These last two relations are not independent if the cloud is near being in virial equilibrium:

$$-E_{\rm G} \sim 2E_{\rm kin} \qquad \text{(thermal + turbulent)}$$

$$\begin{aligned} \frac{GM^2}{R} &\sim M\Delta v^2 \\ \Rightarrow \Delta v &\sim \left(\frac{M}{R}\right)^{1/2} \\ &\sim R^{0.425}, \end{aligned}$$

this is the second Larson relation, and the exponent agrees with the observationally determined one within the rather large error bars

Distribution of clump masses

- clump mass spectrum

$$\frac{dN}{dM} \propto M^{-\gamma},$$

where γ varies from cluster to cluster with $\gamma \sim 1.7 \pm 0.1$

  - most of the mass is in massive clumps

$\Rightarrow$ most stars form in massive clumps

$\Rightarrow$ most stars form in stellar clusters

- this is different from the stellar mass spectrum

$$\frac{dN_\star}{dM_\star} \propto M_\star^{-2.35} \qquad \text{(Salpeter 1955)}$$

$\Rightarrow$ most stellar mass in low-mass stars

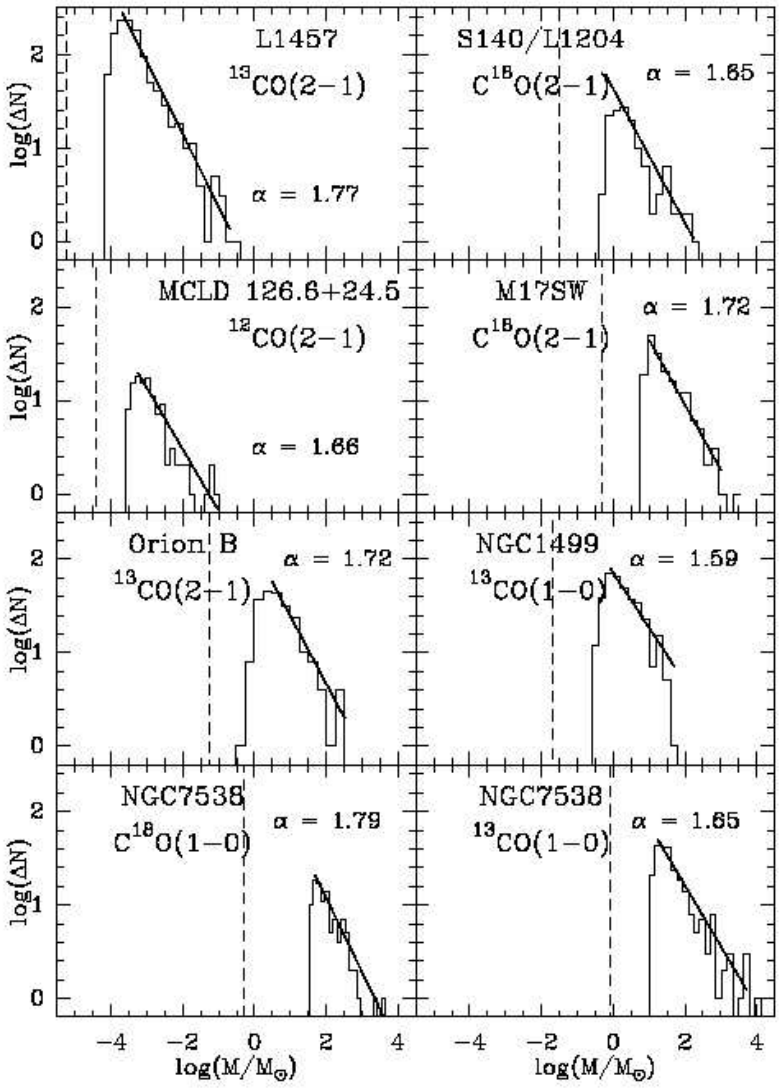

Fig. 6. Clump mass spectra of the eight data sets we analyzed. All spectra are fitted by a power law function $dN/dM \propto M^{-\alpha}$. The straight line represents the best linear fit over the range of masses spanned by the line. The resulting indices α lie in the range 1.59 to 1.79. The minimum possible mass M_{min}^{limits}, given by the resolution limits and the rms noise, is denoted by a dashed line for each data set.

(Kramer, C., Stutzki, J., Rohrig, R., & Corneliussen, U. 1998, A&A, 329, 249)

This is a truly remarkable dynamic range over which there is a power law describing the cloud and clump mass functions:

- from clouds as large as $10^4 M_\odot$ to clumps as small as $10^{-3} M_\odot$

$\Rightarrow$ clouds are scale free over this range

Well, not quite . . .

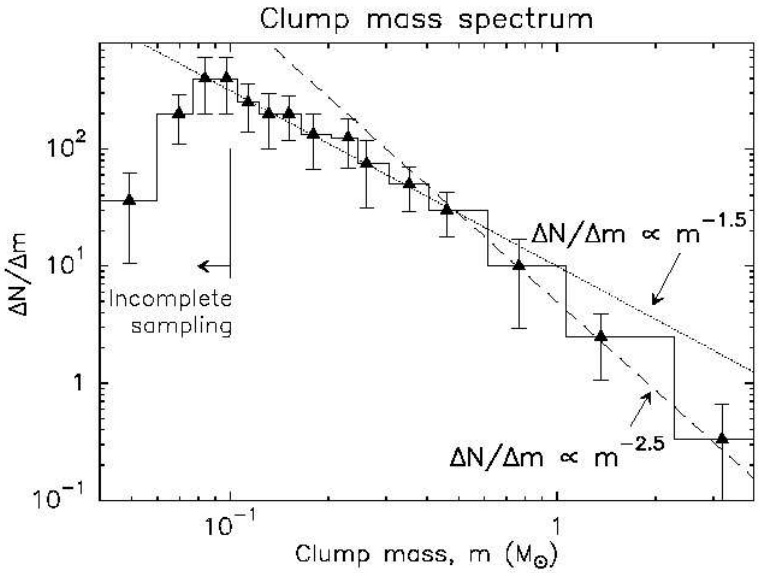

Fig. 5. Frequency distribution of masses for 60 small-scale clumps extracted from the mosaic of Fig. 1 (solid line). The dotted and long-dashed lines show power laws of the form $\Delta N/\Delta m \propto m^{-1.5}$ and $\Delta N/\Delta m \propto m^{-2.5}$, respectively. The error bars correspond to $\sqrt{N}$ counting statistics.

(Motte & Andre, 1998, A&A, 336, 150)

Core Mass Spectrum

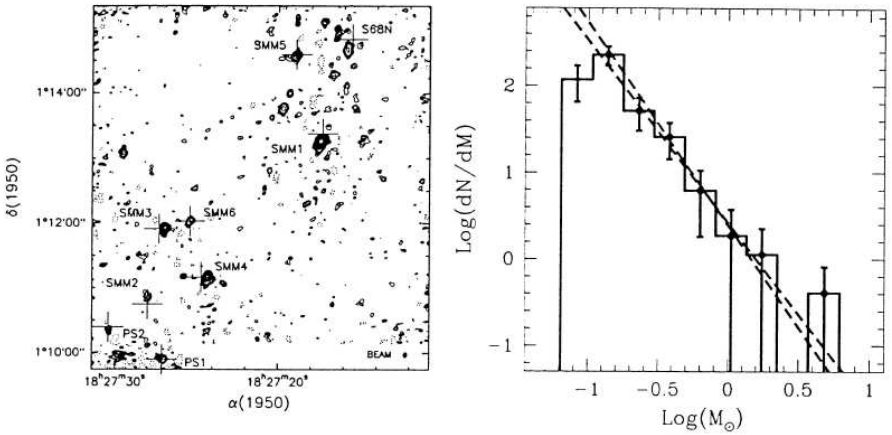

Figure 4. 3-m continuum emission in the Serpens molecular cloud (from Testi and Sargent 1998). This map is the result of a mosaic of 50 fields using the OVRO interferometer. The synthesized beam is $5.7'' \times 4.3''$ (FWHM) and is indicated by the filled ellipse in the lower right corner. The noise level is $\sigma = 0.9$ mJy beam^{-1} and contours begin and are in steps of 3σ. A large number of sources, each a dense dust condensation, are visible. The previously known far infrared and submillimeter sources are marked with crosses and labeled. The core mass spectrum has a slope $dN/dM \propto M^{-2.1}$ and more closely resembles the Salpeter IMF than the clump mass spectrum in molecular clouds.

(Williams, J. P., Blitz, L., & McKee, C. F. 2000, Protostars and Planets IV, 97)

Core mass spectrum

Thus, the core mass spectrum appears to mimic that of the IMF:

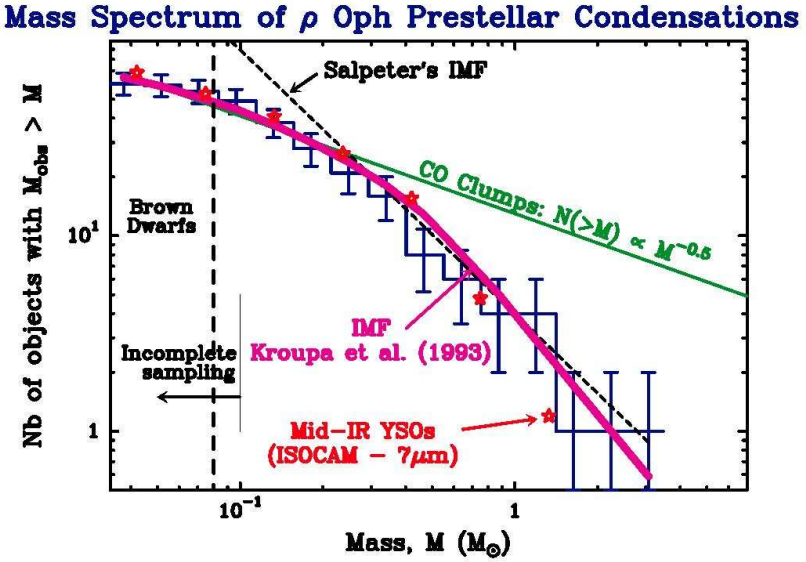

(Pudritz 2002, Science, 295, 68)

- strongly suggests that the form of the IMF may be determined by prestellar core formation

Support in molecular clouds

- molecular clouds exist for ~ 10 free fall times:

$$t_{\rm ff} = \left(\frac{3\pi}{32 G \rho}\right)^{1/2} = 3.4 \times 10^7 n^{-1/2} \text{ years}$$

  For large-scale mean density $\sim 50 \text{cm}^{-3}$,
  $t_{\rm ff} \sim 5 \times 10^6$ years $\sim 0.1\ t_{\rm cloud}$
  clouds require support

- maximum age of stars still associated with molecular clouds is 2–4×10^7 years

- thermal support? No: $c_s \ll \Delta v$

- turbulence? Δv is large enough
  - but motions are supersonic
    - $\rightarrow$ expect shocks
    - $\rightarrow$ shocks should dissipate turbulence

- magnetic fields to cushion shocks?
  equipartition between kinetic and magnetic field energy needed
  - Alfven speed $v_A \sim \Delta v$

$$v_A^2 = \frac{B^2}{8\pi\rho}$$

  $\Rightarrow$ requires $B \sim 25 \mu G$, similar to what is observed

  however, all current MHD simulations suggest that turbulence still decays rapidly (no more than a factor of 2 slower than the non-magnetic case)

$\Rightarrow$ since it is observed, turbulence must be continuously driven:
  - stellar winds?
  - jets and outflows?
  - galactic shear?

Gravitational Collapse

Two different possibilities for pre-collapse conditions:

- quasi-static, near equilibrium
  - centrally condensed
  - roughly spherical
- dynamic, non-equilibrium
  - near uniform density
  - irregular structure
  - "triggered collapse"

(Vanhala, H. A. T. & Cameron, A. G. W. 1998, ApJ, 508, 291)

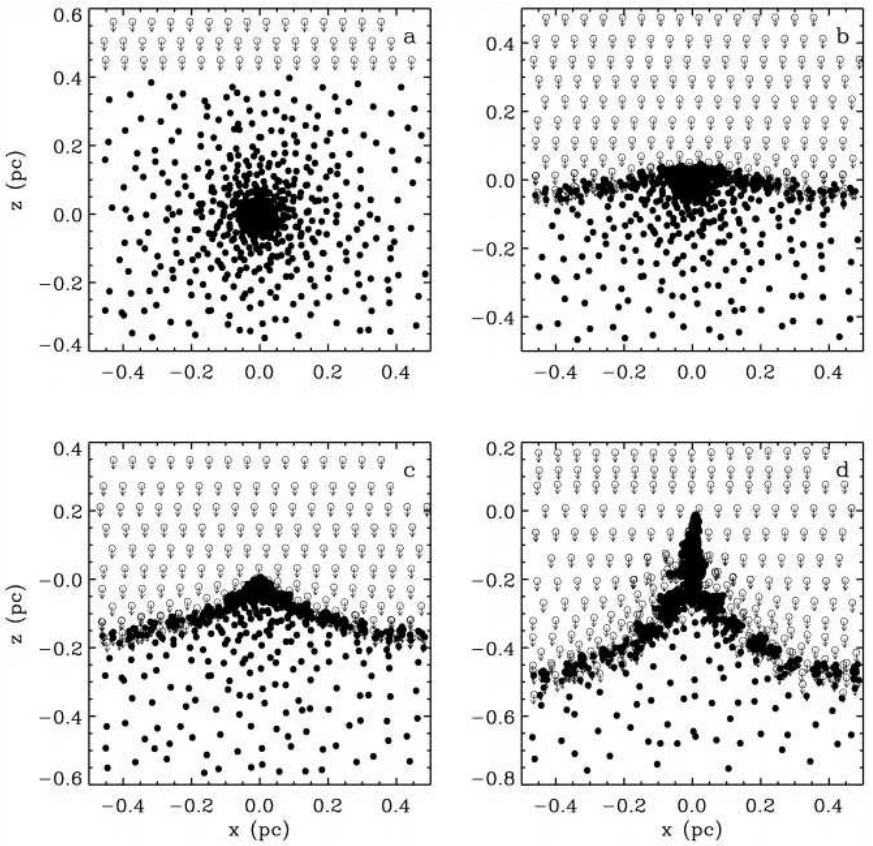

Interaction between the shock wave and the molecular cloud core in a simulation run with 4496 particles in the core and 7772 in the shock wave. The shock wave material is denoted by open circles, and the cloud material by large dots. The initial peak density in the core is 7.35 10-17 g cm-3, and the shock velocity is 25 km s-1. The system is shown in the (x, z)-plane with the units in parsecs. The different frames correspond to (a) t = 0, (b) 21,000 yr, (c) 27,000 yr, and (d) 42,000 yr.

Summary of results of simulations

Adiabatic exponent γ	Shock strength	Result
1	Momentum $\leq 0.1 M_\odot$ km/s	No collapse
	Momentum $\geq 0.1 M_\odot$ km/s	Collapses
$\frac{5}{3}$	All velocities	no collapse; cloud shredded
self-consistent	velocity $<$ 20 km/s	May collapse
	velocity $=$ 20–45 km/s	Collapses
	velocity $\geq$ 45 km/s	Cloud shredded apart

$\Rightarrow$ "Molecular clouds can be triggered into collapse if the momentum of the shock wave is sufficient to compress the core to the point of collapse but not so high that the core will be torn apart."

Gravitational Collapse

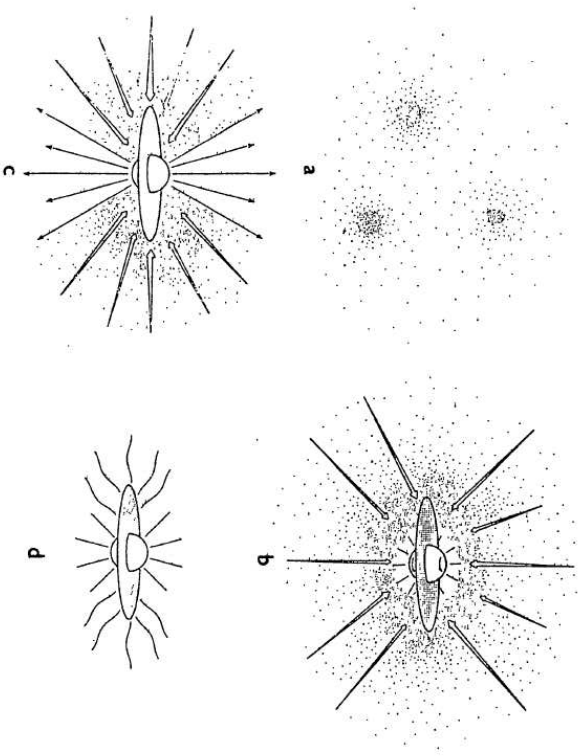

Figure 7 The four stages of star formation. (*a*) Cores form within molecular clouds as magnetic and turbulent support is lost through ambipolar diffusion. (*b*) A protostar with a surrounding nebular disk forms at the center of a cloud core collapsing from inside-out. (*c*) A stellar wind breaks out along the rotational axis of the system, creating a bipolar flow. (*d*) The infall terminates, revealing a newly formed star with a circumstellar disk.

(Shu, F. H., Adams, F. C., & Lizano, S. 1987, ARA&A, 25, 23)

Hydrostatic Disguise?

Ballesteros-Paredes, Klessen, and Vázquez-Semadeni (2003) have recently shown molecular cloud cores may not be in near hydro-static equilibrium [Bonnor-Ebert (BE) spheres]

Analysing 3D SPH simulations of star formation, they found that satisfactory BE profile fits to the column densities could be performed for clumps which were not close to being in hydro-static or thermal equilibrium.

Klessen et al. (2003, "Paper II") also show that such cores in the simulations can also have velocity structures normally associated with hydro-static configurations.

Collapse of a static, dense (spherically symmetric) molecular cloud core

Assume the following:

- thermal support only
- no rotation
- no turbulence
- no magnetic field

Can start with different initial density profiles:

- uniform density
- singular isothermal sphere ($\rho \propto 1/r^2$)
- intermediate density profiles
  - Bonner-Ebert spheroids
  - Gaussian profiles

Collapse of a uniform density, isothermal molecular cloud

(Larson, R. B. 1969, MNRAS, 145, 271)

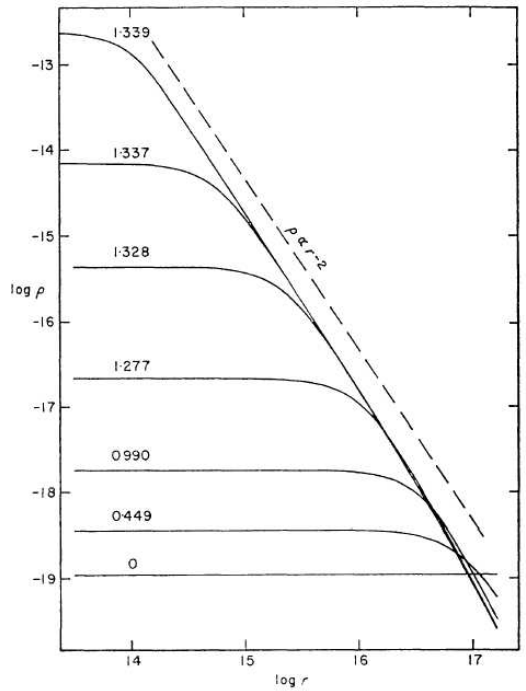

FIG. 1. *The variation with time of the density distribution in the collapsing cloud (CGS units). The curves are labelled with the times in units of* 10^{13} *s since the beginning of the collapse. Note that the density distribution closely approaches the form* $\rho \propto r^{-2}$.

$\Rightarrow$ Density approaches $\rho \propto 1/r^2$ profile

Stable and unstable **Bonnor-Ebert spheres**

(Shu, F. H. 1977, ApJ, 214, 488)

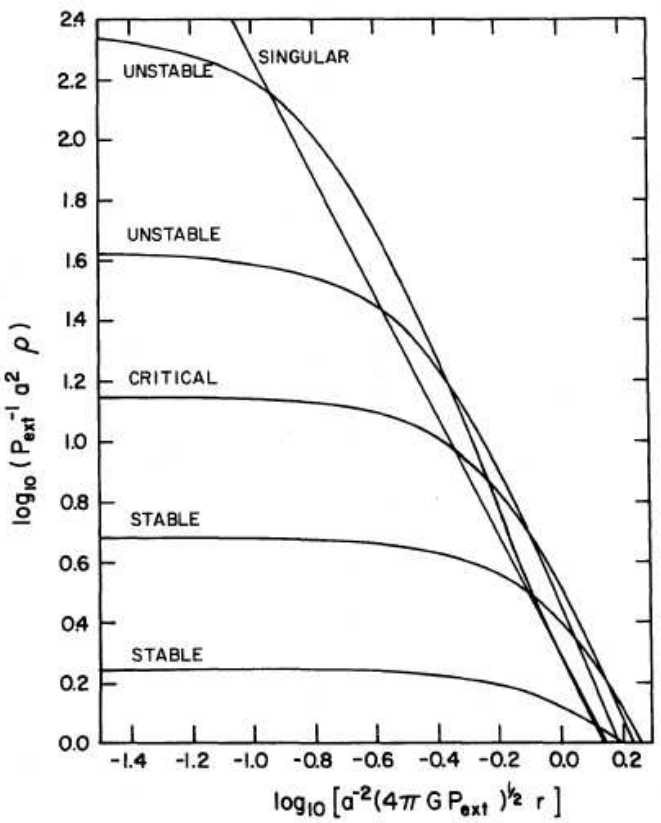

FIG. 1.—Density distributions of bounded isothermal spheres. The outer radius of each sphere is given by the intercept of the corresponding curve with the abscissa. The curve marked "critical" denotes the sphere with the maximum mass consistent with hydrostatic equilibrium at a given external pressure. Hydrostatic spheres which are less centrally concentrated than the critical Bonnor-Ebert state are gravitationally stable; those which are more centrally concentrated are gravitationally unstable. In the limit of infinite central concentration, the latter spheres approach the singular solution.

Collapse of a singular isothermal sphere

- Starts with $\rho \propto r^{-2}$ density profile (Shu, 1977)
- Collapse occurs from "inside-out", i.e., denser regions collapse first, expansion/rarefaction wave travels outward
- mass of central object increases linearly with time

$$\dot{M} = 0.975 \frac{c_s^3}{G}$$

  - essentially this model is a constant accretion rate solution of matter onto a central object

It is *possible* that such initial conditions can arise in quasi-static, pressure supported cores (Bonnor-Ebert spheroids) or through ambipolar diffusion, although the diffusion timescale may be too short

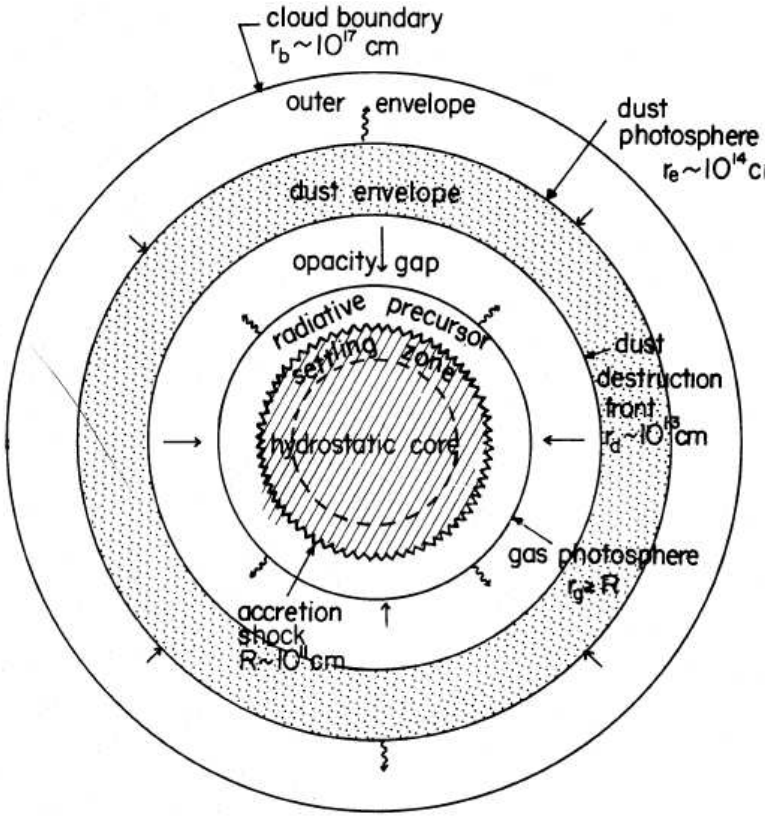

Structure of a spherical protostar during the steady accretion phase with the radii of specific layers approximately indicated (Stahler, S. W., Shu, F. H., & Taam, R. E. 1980, ApJ, 241, 637)

Accretion onto a protostellar core

Initial Conditions:

- uniform density, static
  - $\rho \propto r^{-2}$ when protostellar core forms
  - but velocities are non-zero, *unlike* singular isothermal sphere
  - accretion rate not constant, decreases with time
  - collapse is still "inside-out"
- moderate amount of initial condensation (Bonnor-Ebert spheroids, Gaussian profiles)
  - relatively uniform-density central regions, $\rho \propto r^{-2}$ outer regions
  - accretion rate also decreases with time

Thermodynamics of collapse

- All previous discussions were for an isothermal gas
- Whether the collapse is isothermal or adiabatic determines the nature of the collapse
  Consider the Jeans mass: $M_J \propto T^{3/2}\rho^{-1/2}$
  - assuming $P \propto \rho^\gamma$ (polytrope) $\Rightarrow T \propto \rho^{\gamma-1}$, so $M_J \propto \rho^{(3\gamma-4)/2}$

    $\gamma < 4/3$: collapse without limit

    $\gamma > 4/3$: collapse can be halted, formation of hydrostatic core

The relative heating and cooling rates determine γ

Thermodynamics of collapse

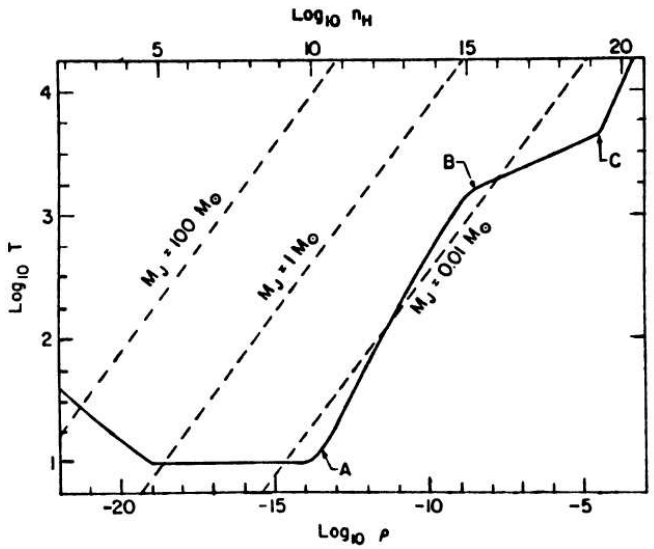

Fig. 3. The evolution in the (log ρ, log T) plane of a protostar in the initial phase of collapse (from Tohline, J. E. 1982, Fund. Cosmic Phys., 8, 1.) Point A indicates the beginning of the adiabatic collapse phase, point B the onset of molecular dissociation, and point C the completion of dissociation. Dashed lines represent loci of constant Jeans mass.

(Bodenheimer, P. 1993, Reviews of Modern Astronomy, 6, 233)

Phases of collapse

- Phase 1: Isothermal Collapse
  - densities: 10^{-19}–10^{-14} g/cm^3
  - optically thin
  - grain cooling balances compressional heating
  - isothermal $\Rightarrow \gamma = 1$
- Phase 2: Formation of Opaque Core
  - densities: 10^{-13}–10^{-9} g/cm^3
  - optically thick to infrared radiation from dust grains
  - $\sim$ adiabatic core of molecular hydrogen: $\gamma = 7/5$
  - core is quasi-hydrostatic, not collapsing
  - core accretes mass and contracts

- Phase 3: Second dynamic collapse
  - densities: 10^{-9}–10^{-3} g/cm^3, T 2000–5000 K
  - at $T \sim 2000$ K, H_2 begins to dissociate
  - energy of collapse goes into dissociation, not heating, so γ is reduced: $\gamma \sim 1.1$
- Phase 4: Formation of Second Hydrostatic (Stellar) Core
  - densities: $\gtrsim 10^{-3}$ g/cm^3, $T \gtrsim 5000$ K
  - H_2 completely dissociated, $\sim$ ideal, monatomic gas
  - optically thick, adiabatic $\Rightarrow \gamma = 5/3$
- Phase 5: Main Accretion Phase
  - accretion of infalling gaseous envelope
  - remnants of first core disappear
  - protostar begins to burn deuterium

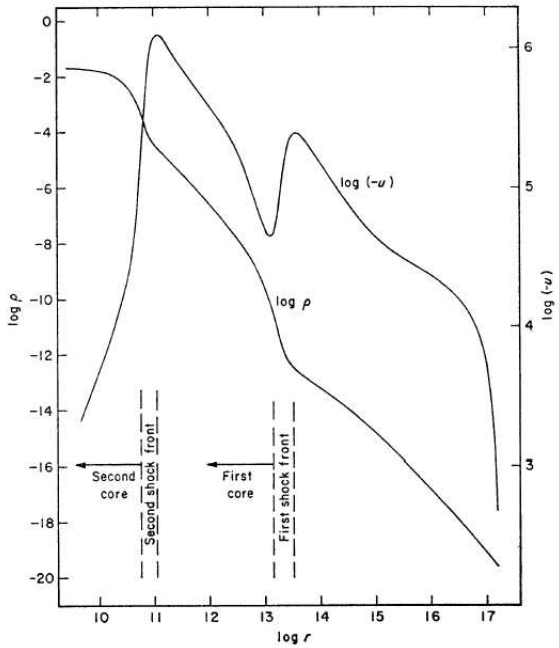

FIG. 2. *The density and velocity distributions at a time shortly after the formation of the second (stellar) core (CGS units). The shock fronts are represented by the regions of steep positive slope in the velocity curve.*

(Larson, R. B. 1969, MNRAS, 145, 271)

Observational evidence of initial conditions

- Density profiles of pre-stellar cores
  - $\rho \propto r^{-2}$ at large radii ($r \gtrsim 3000$ AU)
  - flatter in the centre ($\rho \propto r^{\alpha}$ with $\alpha = -0.4$ to -1.2)
- Energy of outflows observed to decrease with age
  - outflows thought to be correlated with accretion
    $\Rightarrow$ accretion rate decreases with time
  - This can be explained if the pre-collapse clouds are not very centrally condensed
- Thus, the initial conditions appear to be closer to the uniform-density case than the singular isothermal sphere case

spherical accretion

- may be an appropriate description far from the accretion centre
- breaks down in the vicinity of the protostar (unless the accreted material literally has zero angular momentum)
- therefore, the preceding picture of accretion directly onto the surface of the protostar must be modified

This naturally leads us to consider...

Discs and outflows around young stars

- not just important in star formation
  - mass-transferring binaries
    - cataclysmic variables (accretion onto a white dwarf)
    - X-ray binaries (accretion onto a neutron star or black hole)
  - central black holes (AGN/quasars)
- theoretically, they have to exist
  - angular momentum of gas does not allow it to collapse to a point
  - disk must extract angular momentum from gas, allowing it to fall onto the central object

  $\Rightarrow$ most of a star's mass passes through an accretion disk
- observationally, ...

They really do exist!

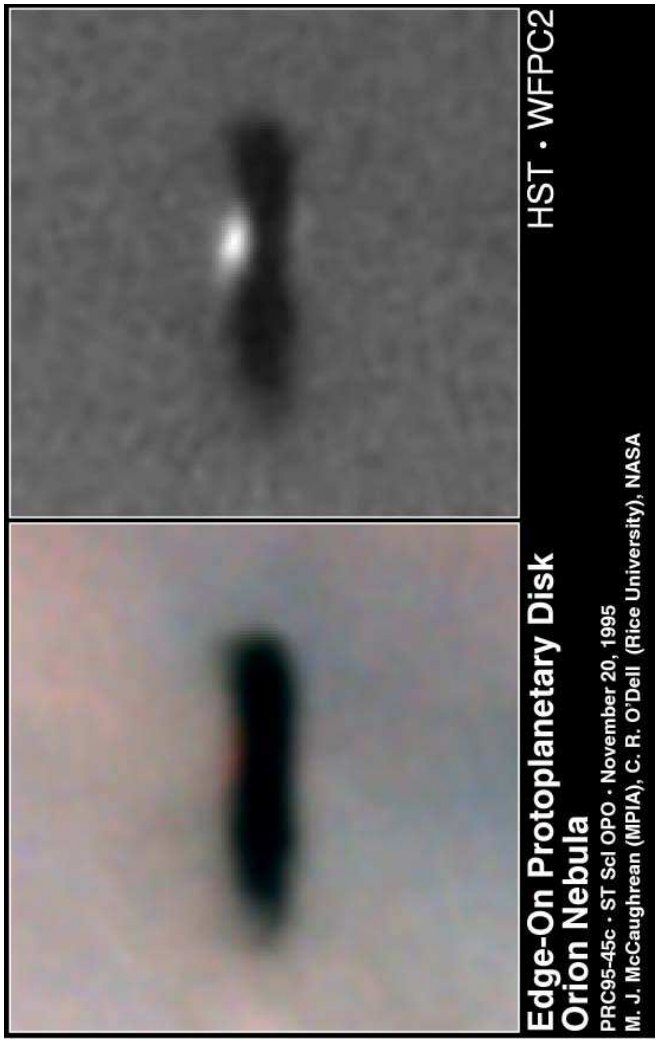

(McCaughrean, M. J. & O'dell, C. R. 1996, AJ, 111, 1977)

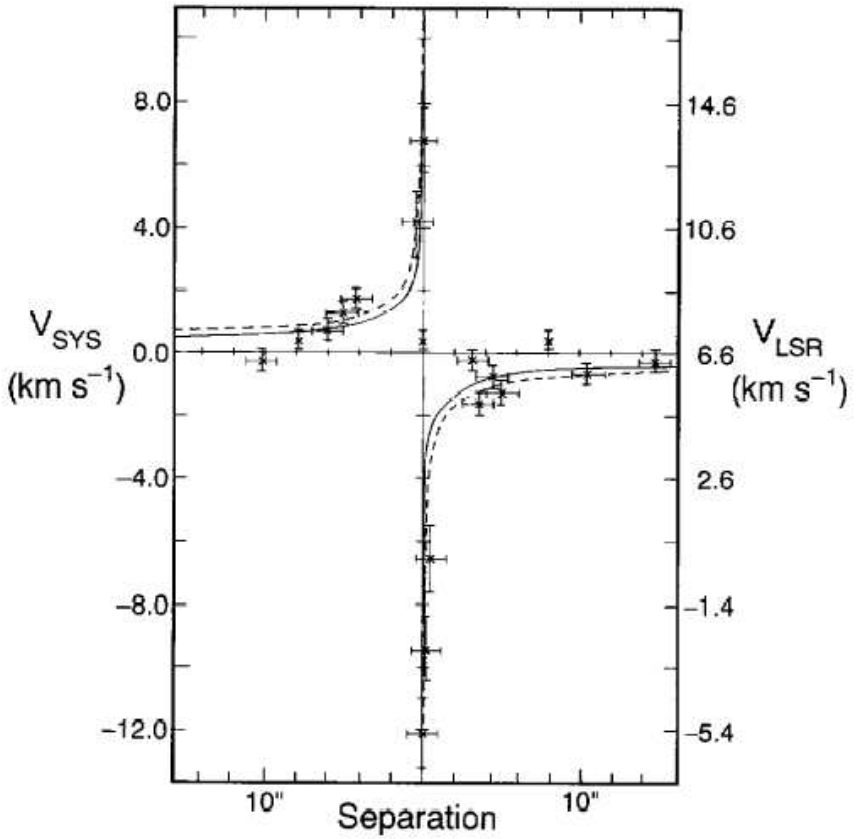

FIG. 3.—The observed rotation curve for HL Tau. Error bars indicate the uncertainties in position and velocity for the data points. The solid and dashed lines show the expected variation of peak position with velocity for material in Keplerian rotation about stars of mass 0.55 and 1 $M_{\odot}$, respectively.

(Sargent, A. I. & Beckwith, S. V. W. 1991, ApJ, 382, L31)

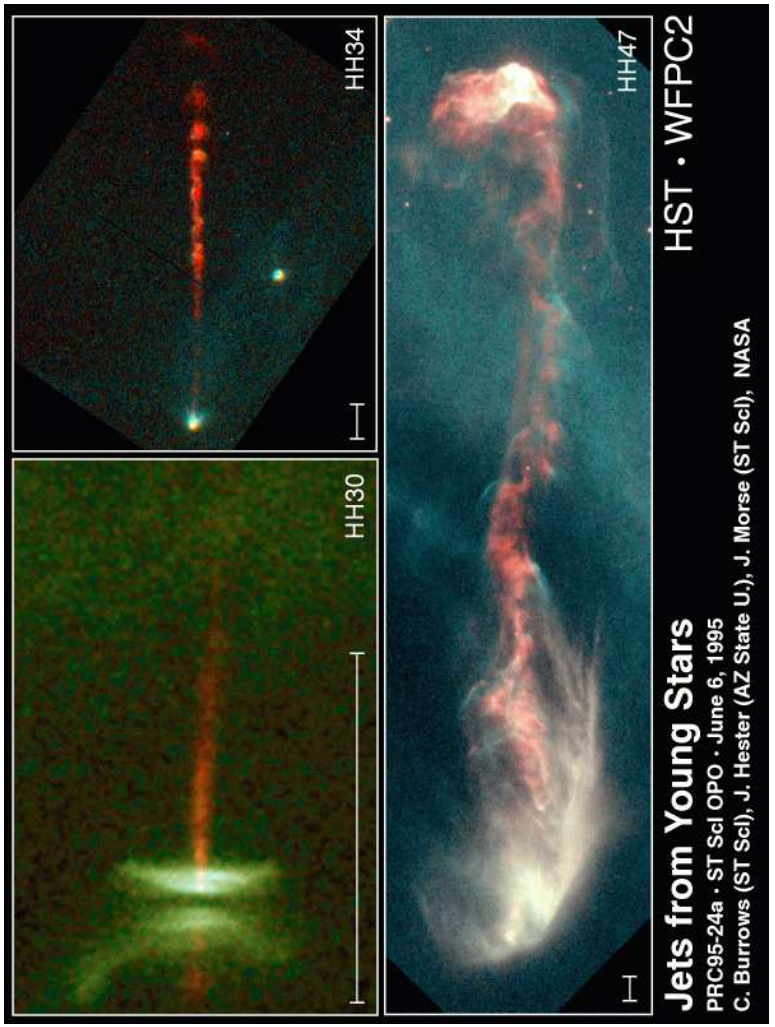

Disc Basics

- Structure of a thin disc: $H \ll r$

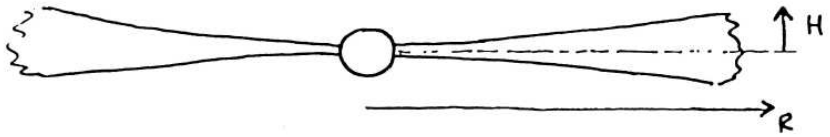

For a vertically isothermal, ideal gas,

$$P \sim c_s^2 \rho, \quad \frac{dP}{d\rho} = -g_z \rho, \quad g_z \approx g_r \frac{z}{r}$$

$$\Rightarrow \rho \approx \rho(r) \exp\left(-\frac{z^2}{2H^2}\right), \quad H \equiv c_s \left(\frac{r^3}{GM_\star}\right)^{1/2}$$

$$\frac{H}{r} = \frac{c_s}{v_\phi}, \quad \text{so} \quad c_s \ll v_\phi$$

- circular velocity very close to Keplerian
  $v_\phi = \Omega r$, $\Omega \equiv \left(\frac{GM_\star}{r^3}\right)^{1/2}$
- local Keplerian velocity is highly supersonic
  Mach number $M \equiv v_\phi / c_s$

Disc basics (cont.)

- effective kinematic viscosity
  $\nu = \alpha c_s H$, where α is a dimensionless parameter and we expect $\alpha \lesssim 1$
  (Shakura & Sunyaev 1973, A&A, 24, 337)
- radial inflow velocity is small
  $v_r \sim \nu / r \sim \alpha c_s H / r \ll c_s$

- viscous timescale $\gg$ dynamical/orbital timescale

$$t_{\rm visc} \sim \frac{r}{v_r} \sim \frac{r^2}{\nu} \sim \frac{P}{2\pi\alpha}\left(\frac{r}{H}\right)^2,$$

where P is the orbital period at radius r

Result of viscous evolution

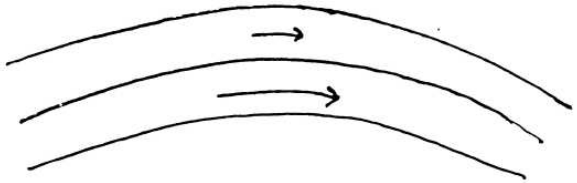

- disc rotates differentially ($\Omega \propto r^{-3/2}$), contains shear motions
- viscous coupling at neighboring radii (annuli) attempts to reduce shear

  $\Rightarrow$ speeds up outer annulus, slows down inner one
- angular momentum transferred outward
- inner annulus moves inward, outer annulus moves outward

Final state

- 'all' the mass winds up in the centre
- 'all' the angular momentum transferred out to infinity

Viscous diffusion of a ring of matter

- mass is transferred inward
- angular momentum is transferred outward
  - "all" the matter winds up at the origin
  - "all" the angular momentum is transferred out to infinity

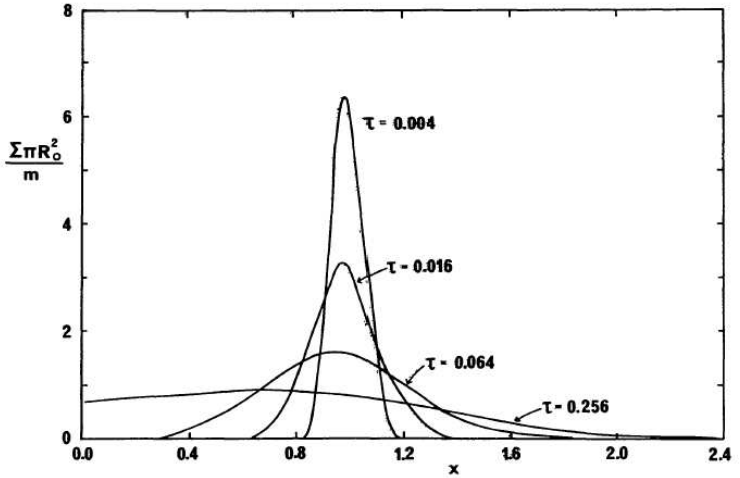

Figure 1 The viscous evolution of a ring of matter of mass m. The surface density Σ is shown as a function of dimensionless radius $x = R/R_0$, where R_0 is the initial radius of the ring, and of dimensionless time $\tau = 12\nu t/R_0^2$ where ν is the viscosity.

(Pringle, J. E. 1981, ARA&A, 19, 137)

Similarity solution for an evolving disc

(Lin, D. N. C. & Pringle, J. E. 1987, MNRAS, 225, 607)

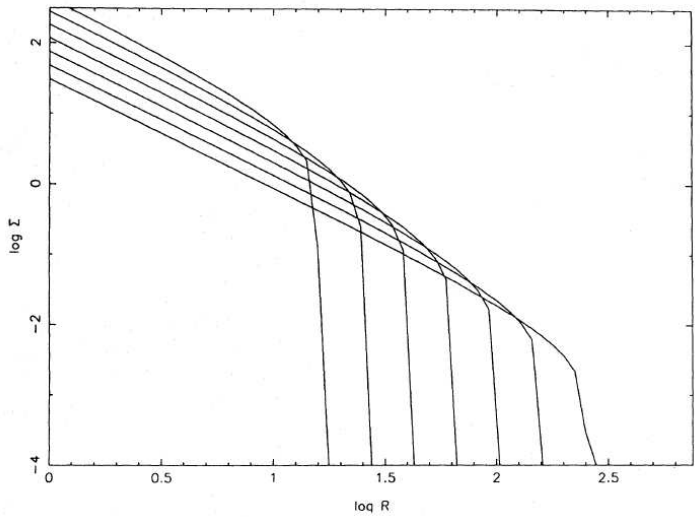

Figure 1. A log–log plot of surface density Σ versus radius R for the similarity solution given by equations (3.3) and (3.4). Σ and R are in arbitrary units. The outer disc radius increases with time, and time increases by a factor of $\sqrt{10}$ for each model.

- outer edge of disc expands
- matter is accreted onto the central point

Source of viscosity?

- normal kinematic viscosity
  - far too small in protostellar discs
- turbulent convection
  - magnitude of effective (turbulent) viscosity small, disc may not be unstable to convection
- magneto-hydrodynamic turbulence (Balbus-Hawley instability)
  - looks promising

Non-local angular momentum transport mechanisms

- spiral shock waves (induced via a companion)
- gravitational torques (discs must be self-gravitating, massive)
  - disc develops spiral density waves
  - very efficient ($\alpha > 1$)

MHD turbulence

- presence of even a weak magnetic field leads to
  - a magneto-rotational instability

  - field perturbed radially
  - field tries to enforce rigid location
  - angular momentum transferred outward
  - field displaced farther outward
  - instability grows rapidly
- effective value of α in the range 0.05–0.1
  - assumes flux freezing
- depends on the ionisation fraction
  - α may be much less than flux freezing case
  - may lead to a 'dead' zone inside the disc where the ionisation fraction is low

Disc/star interface

- Boundary layer
  - disc joins continuously to star
  - star expected to be rotating near breakup
  - if star is not rotating at breakup, i.e., $\Omega_\star < \Omega_{\rm Kep}$, then there is a boundary layer in which the gas is slowed down:

$$L_{\rm BL} = \frac{1}{2}\dot{M}\left(\Omega_{\rm Kep}^2 - \Omega_\star^2\right) R_\star^2$$

$$L_{\rm BL} \approx \frac{1}{2}\frac{GM_\star\dot{M}}{R_\star}, \text{ for } \Omega_{\rm Kep}^2 \gg \Omega_\star^2$$

  $\Rightarrow$ up to half the accretion energy can be release in the boundary layer, producing UV excess
- Disc truncated by magnetic field
  - gas from disc falls onto star along field lines
  - gas lands near the poles in 'hot spots', emitting UV radiation

Disc/star interface (cont.)

- observations of CTTS show rapidly infalling gas
  - velocity of gas provides constraints on the star's parameters: $v \approx \left(\frac{2GM_\star}{R_\star}\right)^{1/2}$
- T-Tauri stars not observed to be rotating near break-up ($P_{\rm breakup} \approx 0.1$ days)
  - Classical T-Tauri stars $P \approx 8$ days
  - Weak-line T-Tauri stars $P \approx 2$ days
- magnetic field allows star to be anchored to disc
- strength of the magnetic field determines the corotation radius, and therefore the rotation rate of the protostar
- with observed fields of ~ 1 kG, the central star would have a equilibrium rotation rate of ~ 10 days
- when disc is later dispersed, star can contract and spin up to $P \sim 2$ days

FU Orionis Systems

- young stars which undergo rapid increases in luminosity, ~ 4 mags
  - outbursts last ~ 100 years
  - attributed to an increase in accretion ($\gtrsim 10^{-4} M_\odot$/yr)
  - $\sim 0.01\, M_\odot$ accreted per outburst!
  - each star estimated to undergo ~ 10 outbursts

  $\Rightarrow$ a significant fraction of a star's mass can be accreted in the FUOR outbursts
- observations of FUORs
  - disc outshines star—easy to study disc
  - double-peaked absorption lines from rotating accretion disc

Schematic Model of an FU Orionis System

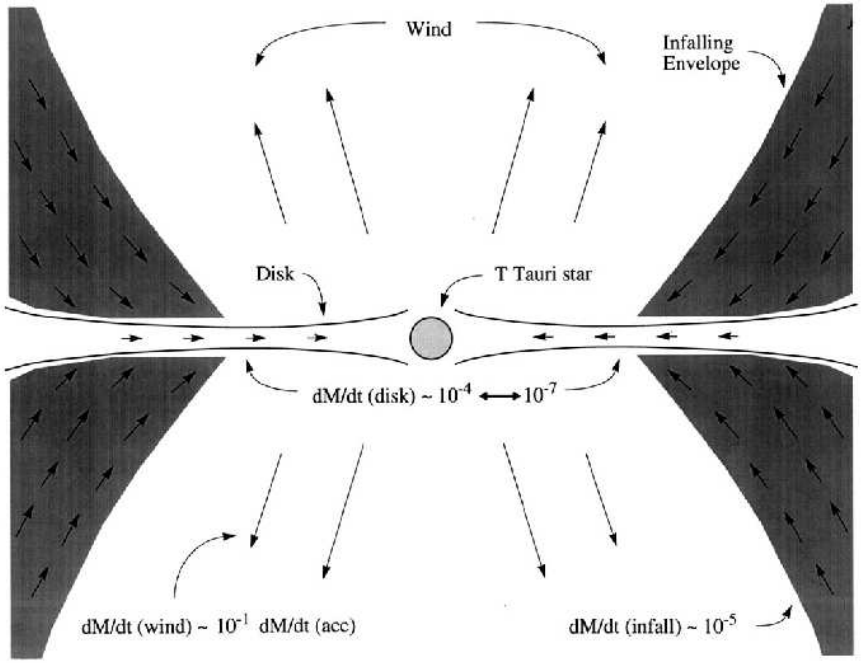

Figure 1 Schematic picture of FU Ori objects. FU Ori outbursts are caused by disk accretion increasing from $\sim 10^{-7}\ M_\odot\ \mathrm{yr}^{-1}$ to $\sim 10^{-4}\ M_\odot\ \mathrm{yr}^{-1}$, adding $\sim 10^{-2}\ M_\odot$ to the central T Tauri star during the event. Mass is fed into the disk by the remanant collapsing protostellar envelope with an infall rate $\lesssim 10^{-5}\ M_\odot\ \mathrm{yr}^{-1}$; the disk ejects roughly 10% of the accreted material in a high-velocity wind.

(Hartmann, L. & Kenyon, S. J. 1996, ARA&A, 34, 207)

FU Orionis Systems

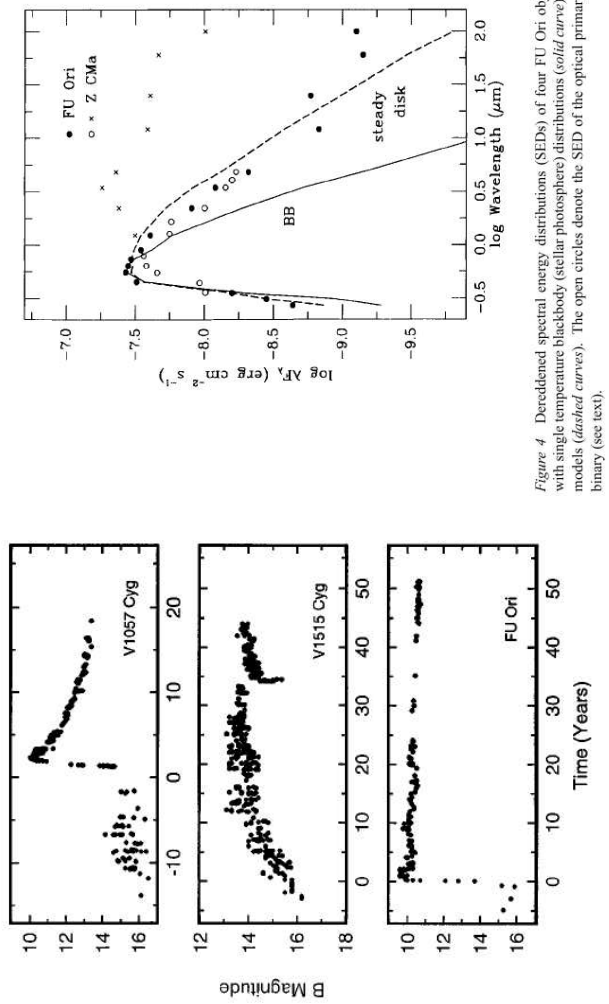

Figure 4 Dereddened spectral energy distributions (SEDs) of four FU Ori objects, compared with single temperature blackbody (stellar photosphere) distributions (*solid curve*) and steady disk models (*dashed curves*). The open circles denote the SED of the optical primary of the Z CMa binary (see text).

(Hartmann, L. & Kenyon, S. J. 1996, ARA&A, 34, 207)

Mechanisms for increased accretion rate

- thermal instability in the accretion disc
- gravitational instabilities are potentially important since the disks should be massive
- passage of a close companion star near the disc
- material piles up behind a planet in the disc until the gas becomes unstable

Outflows from young stars

- Two kinds of outflow
  - Jets
    - highly collimated
    - high velocity (≈ 400 km/s)
    - believed to be 95–99% neutral gas
    - densities $\sim 10^3$ cm^{-3}
    - can be up to 10 pc long
    - contain Herbig-Haro objects (optical emission from bow shocks)
  - Outflows of molecular gas
    - poorly collimated
    - lower velocity (≈ 100 km/s)
    - dynamical times 10^4 – 10^5 years
    - believed to be driven by the jet
- both outflows are bipolar
- time evolution
  - power in jets/outflows decreases with time
  - opening angle of outflow thought to increase with time

Relationship between outflows and jets

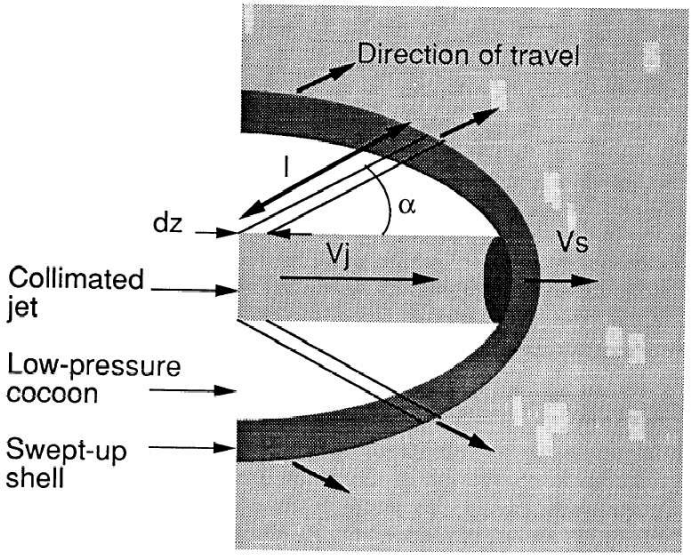

FIG. 3.—Cross section of bow shock geometry and shell of swept-up material for a radiative shock. The pressure generated in the shocks is rapidly dissipated near the jet head, so the cocoon has negligible pressure far from the jet head. Away from the jet head, the cooled, shocked material sweeps up a dense shell in a momentum-conserving snowplow phase.

(Masson, C. R. & Chernin, L. M. 1993, ApJ, 414, 230)

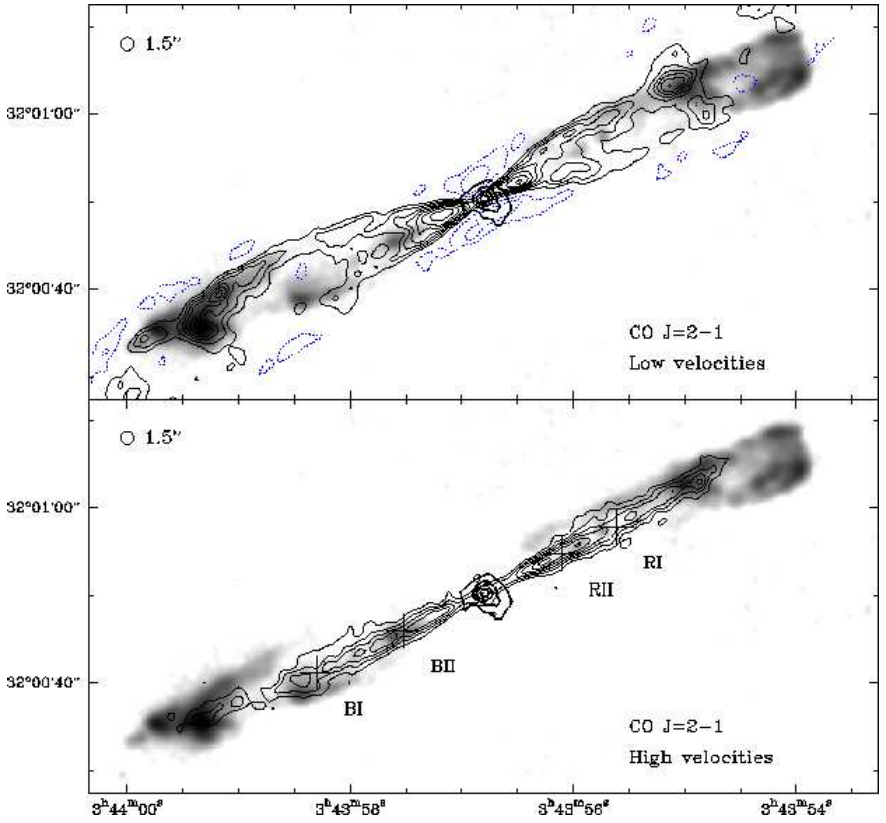

CO J = 2 → 1 emission (thin contours) integrated in two different velocity intervals and superimposed on the H2 v=1-0 S(1) emission (greyscale; from McCaughrean et al. 1994) and the 230 GHz continuum emission (thick contours; contours are 10, 30, 50 and 70 mJy/beam). The angular resolutions are for the H2, at PA for the CO, and at PA for the continuum observations. For clarity, the noise at the edges of the mosaic has been masked. Upper panel: CO emission integrated between LSR velocities 2.2 and 18.2 km/s (the systemic velocity is 9.2 km/s); contours are 1.6 Jy km/s/beam. Lower panel: CO emission integrated for velocities lower than 2.2 km/s and larger than 18.2 km/s; first contour is 1 Jy km/s/beam and contour step is 1.5 Jy km/s/beam.

(Gueth, F. & Guilloteau, S. 1999, A&A, 343, 571)

Links between accretion and outflow

- well-developed theoretical ideas linking mass loss from outflows with disc accretion
- observationally ...
  - correlation between bolometric luminosity of deeply embedded objects (mostly accretion luminosity) with power of CO outflows
  - mass loss from outflows $\sim 10^{-6} M_\odot$/yr
  - accretion rate to form a solar-mass star during embedded phase $\sim 10^{-5} M_\odot$/yr

  $\Rightarrow \dot{M}_{\rm wind} \sim 0.1\, \dot{M}_{\rm acc}$
- since outflow power is observed to decrease with time, we infer that the accretion also decreases with time

Theories for jets

- high velocities ($\sim$ escape velocity at star's surface) imply that jets are formed deep in the potential well
- models of Blandford & Payne (1982)
  - disc threaded by poloidal field
  - material accelerated along field lines by centrifugal forces
  - jet collimated by toroidal magnetic field
- disc wind model (e.g., Pudritz et al. models)
  - disc wind generated at range of radii
  - jet from inner region
- wind perhaps generated by strong gradients in magnetic pressure close to star/disc boundary
- Shu et al. model
  - jet originates at magnetic field cusp
  - cusp occurs in the boundary between star and disc
  - or at inner edge of magnetically truncated disc

Driving Jets

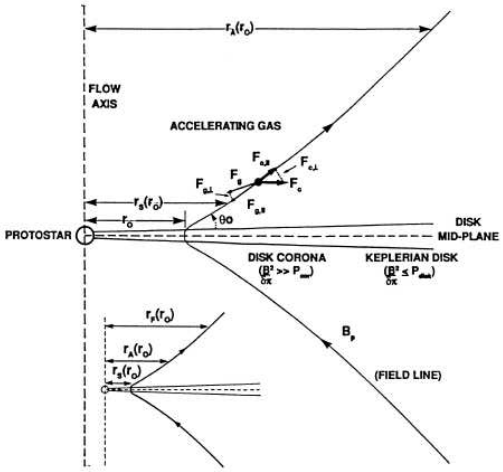

Figure 3. Structure of a protostellar accretion disk, its threading magnetic field, and the associated hydromagnetic disk wind

(Pudritz, R. E., Pelletier, G., & Gomez de Castro, A. I. 1991, NATO ASIC Proc. 342: The Physics of Star Formation and Early Stellar Evolution, 539)

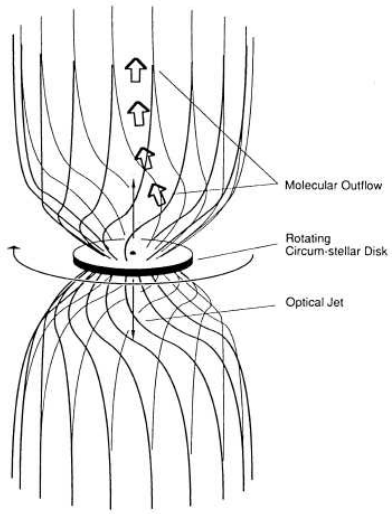

Figure 6. A schematic drawing of the magnetohydrodynamical model.

(Fukui, Y., Iwata, T., Mizuno, A., Bally, J., & Lane, A. P. 1993, Protostars and Planets III, 603)

Theories for Outflows

- May be driven by jet through entrainment of surrounding gas
  - turbulent layer at surface of jet
  - interaction at the bow shock
- in addition to jet, there may be a low-velocity disc wind
- outflow may be collimated by gas in the infalling envelope
  - opening angle observed to widen with time
  - excavated by wiggling jet?
  - excavated by wind?
  - material with higher angular momentum falls in later
    - high angular momentum gas cannot occupy space above poles

    ⇓ expect wider cavity with time

Young Single Stars

- Three observable components:
  - young star
  - circumstellar disc
  - infalling gaseous envelope
- Energy sources
  - contraction and nuclear burning
  - accretion
- spectral energy distribution (SED) depends on the relative importance of these components:

  Star: blackbody spectrum at $T_\star$

  Disc: temperature of disc varies with radius, not a single temperature blackbody

  Envelope: absorbs/re-emits and scatters light
  - very cold
  - long wavelength radiation

Classification of Young Stars

Three main classes based on SEDs: νF_ν versus ν

- Class I
  - protostellar core and disc embedded in infalling envelope
  - most radiation emitted from envelope, seen in infrared
  - luminosity primarily from accretion (not nuclear burning or contraction)
  - ages $\lesssim$ a few times 10^5 years ($\approx t_{\rm ff}$)
- Class II
  - tenuous or no envelope
  - optically visible, with infrared and ultraviolet excesses:
    - IR: cool disc material
    - UV: accretion onto star
  - also known as Classical T-Tauri stars (CTTS)
    - strong emission lines (e.g., Hα) from accretion
  - ages a few times 10^6 years

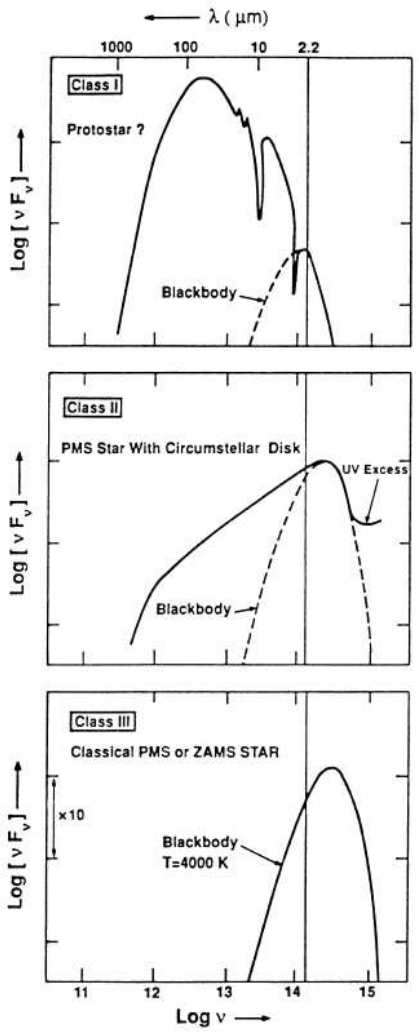

Figure 4. Classification scheme for YSO energy distributions

(Lada, C. J. 1991, NATO ASIC Proc. 342: The Physics of Star Formation and Early Stellar Evolution, 329)

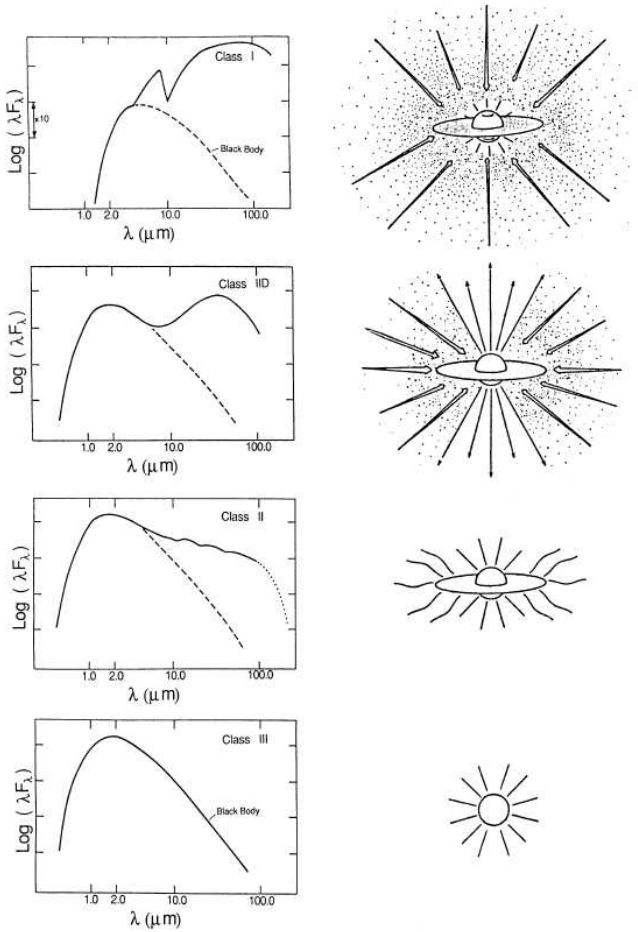

FIG. 4–The quasi-continuous evolutionary sequence of SEDs for low-mass stars proposed by Adams *et al.* (1987). On the left, spectral energy distributions typical of the four morphological classes are shown. The corresponding stages in the pre-main-sequence evolution of a low-mass star are shown schematically on the right. These stages include (1) an accreting protostar (Class I SED), (2) an accreting protostar with a well-developed outflow (Class IID), (3) the T Tauri phase (Class II), and (4) the naked T Tauri or post-T Tauri phase (Class III). Figure adapted from Lada (1987) and Shu *et al.* (1987).

(Wilking, B. A. 1989, PASP, 101, 229)

SEDs of Class II objects

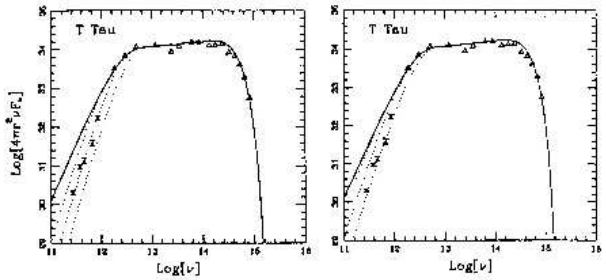

Figure 8. Spectral energy distribution for the flat spectrum class II source T Tauri. The left hand diagram also plots the theoretically derived fits to the SED assuming a circumstellar disk and an opacity law of the form $\kappa_\nu \sim \nu^2$ for disk masses of 0.01, 0.1, 1.0 $M_\odot$(dotted lines) and for infinite disk mass (solid line). The right hand figure plots the same models but with a different opacity law, $\kappa_\nu \sim \nu^{1.5}$. With permission from Adams, Emerson and Fuller (1991).

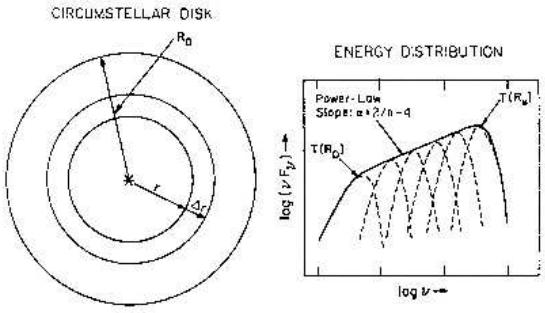

Figure 7. Schematic diagram of an optically thick disk and its emergent spectral energy distribution. The emergent energy distribution is produced by a superposition of blackbodies of appropriately varying temperature. The energy distribution consists of three parts. At high frequencies the emission falls off approximately exponentially appropriate for the Wien side of a Planck curve. At intermediate frequencies the emission follows a power-law form and at the lowest frequencies the emission falls with a slope given by the Rayleigh-Jeans Law or somewhat steeper if the emission becomes optically thin.

(Lada, C. J. 1991, NATO ASIC Proc. 342: The Physics of Star Formation and Early Stellar Evolution, 329)

Classification of Young Stars (cont.)

- Class III
  - disc has been accreted/destroyed
  - only central object is seen
  - $\Downarrow$ blackbody spectrum
  - pre-main-sequence star (PMS), deuterium burning
  - also called weak-line T-Tauri stars (WTTS)
  - do not have strong emission lines
  - ages a few times 10^6 to a few times 10^7 years

Classification of Young Stars (cont.)

- Class 0
  - extreme version of Class I
  - pre-stellar dense molecular cloud cores
    - very cold (15–30 K)
    - near blackbody SED

Finally, the average envelope mass is seen to decrease with class number:

Class 0: $M_{\rm env} \sim 0.2$–$3\,M_\odot$

Class I: $M_{\rm env} \sim 0.02$–$0.3\,M_\odot$

Class II: $M_{\rm env} \lesssim 0.03\,M_\odot$

Pre-main-sequence Stellar Evolution

Evolution from protostar to main-sequence

- evolution in the H-R diagram
  - temperature
  - luminosity
- effects of accretion on H-R diagram evolution
- evolution of a star's spin
  - star-disc locking
  - magnetic braking

Pre-main-sequence Evolution

- protostellar core has $M \ll M_\odot$
- star not in equilibrium
  - accreting gas from disc, surface heated
  - contracting, not in thermal equilibrium
- star is fully convective (on 'Hayashi Line')
- star contracts on the 'Kelvin-Helmholtz' timescale:

$$t_{\rm KH} = \frac{\text{Thermal Energy}}{\text{Energy Loss Rate}} = \frac{GM_\star^2/R_\star}{L_\star}$$
$$\sim 3 \times 10^7 \text{ years} \quad \text{(Solar-type star)}$$

$\Rightarrow$ $t_{\rm KH}$ shorter for higher mass stars

- temperature increases as star contracts
  - virial theorem $\Rightarrow \langle T \rangle \sim \frac{M}{R}$

- When $T_c \approx 10^6$ K, star begins to burn deuterium
  - contraction effectively stopped due to new energy source
- contraction resumes when deuterium exhausted
- eventually, temperature becomes high enough for hydrogen fusion ($T_c \approx 10^6$ K)
  - if $M_\star \gtrsim 0.1\, M_\odot$
- star is now on the zero age main-sequence (ZAMS), and is in thermal equilibrium

Evolution in the H-R Diagram

- young low-mass stars are fully convective
- Hayashi (1961) track
  - evolutionary track for pre-main-sequence star as it contracts toward the main-sequence
  - tracks are nearly vertical in H-R diagram
  - Hayashi track gives lowest $T_{\rm eff}$ for an object in quasi-static equilibrium

  $\Rightarrow$ 'forbidden region' lies to the right of the Hayashi track
- stars with $M \gtrsim 0.5\,M_\odot$ develop radiative cores
- Henyey et al. (1955) track
  - appropriate for radiative (non-convective) objects
  - $\sim$ horizontal in H-R diagram

Actual pre-main-sequence tracks are a combination of the two

Schematic pre-main-sequence track

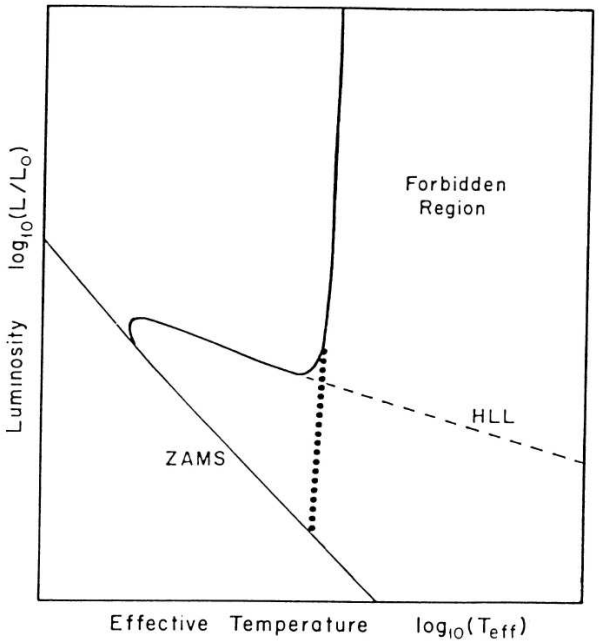

Figure 2. A theoretical PMS track (schematic). A star of a fixed mass is first convective and descends a nearly vertical path, eventually turning onto the more horizontal radiative track discovered by Henyey et al. (1955). The vertical path and its downward extension (dotted line) form the border of the forbidden region of Hayashi (1961).

(Stahler, S. W. & Walter, F. M. 1993, Protostars and Planets III, 405)

Example pre-main-sequence tracks (no accretion)

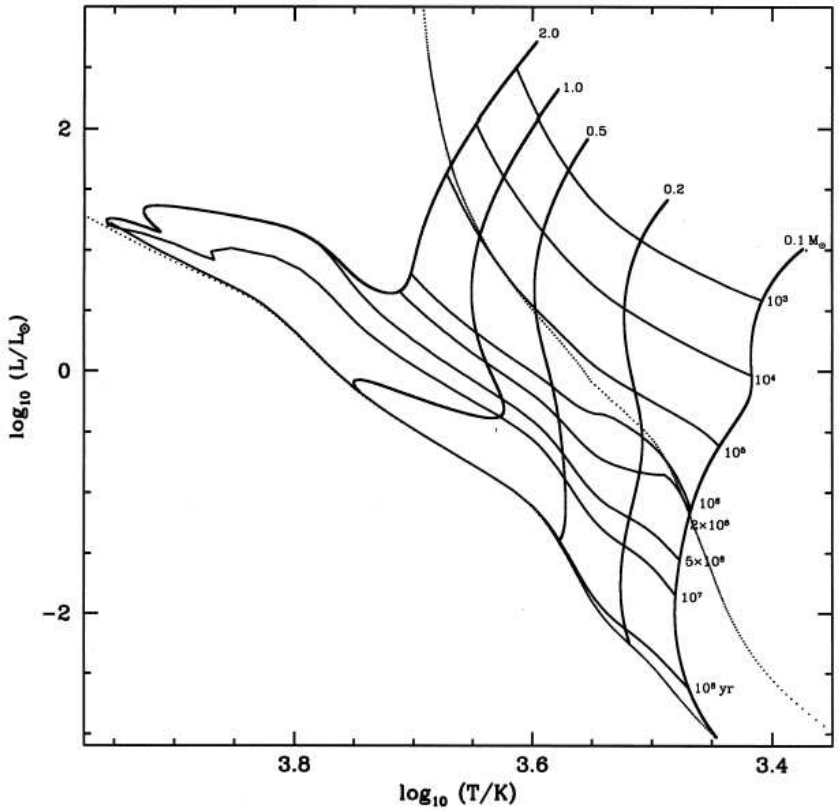

Figure 1. A Hertzsprung–Russell diagram showing constant-mass pre-main-sequence tracks of solar metallicity ($Z = 0.02$) stars in the range 0.1 to 2.0 $M_\odot$. Isochrones of ages ranging from 10^3 to 10^8 yr are drawn across the tracks. The models were begun at radii large enough that these isochrones are not affected by small displacements of this starting point. The zero-age main and deuterium-burning sequences appear as dots logarithmically spaced in mass.

(Tout, C. A., Livio, M., & Bonnell, I. A. 1999, MNRAS, 310, 360)

'The Deuterium Main-Sequence'

- The stellar birthline appears to coincide with the deuterium-burning main-sequence
- 'Explanation'
  - young stars obscured by dusty envelopes
  - onset of deuterium burning somehow creates wind which blows away envelope

  $\Rightarrow$ stars not observed before deuterium-burning stage
- Problem
  - no self-consistent model of how deuterium burning could lead to winds

The Stellar Birthline

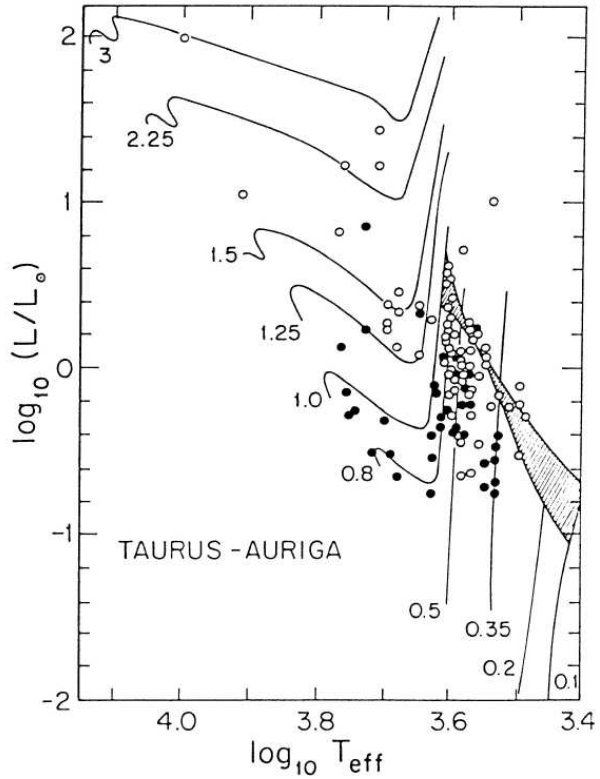

Figure 4. The birthline for low-mass stars (from Stahler 1988).The hatched region shows the variation in the birthline for protostellar mass accretion rates from 2×10^{-6} to 1×10^{-5} $M_\odot$ yr^{-1}. The lighter solid curves are the PMS tracks of Iben (1965), each track labeled by the corresponding mass in solar units. Open circles are observations of CTTS in Taurus-Auriga by Cohen and Kuhi (1979), while filled circles are NTTS from Walter et al. (1988).

(Stahler, S. W. & Walter, F. M. 1993, Protostars and Planets III, 405)

The Stellar Birthline

- Better explanation
  - stars evolve rapidly down Hayashi tracks, unlikely to be seen
  - obscured by envelopes
  - spend a longer time on the deuterium-burning sequence

  $\Rightarrow$ more likely to be seen
  - reasonable chance of envelope being dissipated during this time
  - if stars are still accreting, they will just move along this deuterium-burning sequence (to higher masses)

Pre-main-sequence Evolutionary Tracks

- In theory, placing a pre-main-sequence star on the H-R diagram gives:
  - the star's mass
  - the star's age
- But, it is very difficult to make accurate models of pre-main-sequence stars
  - model atmospheres
    - relatively low temperature
    - molecules
    - dust
    - grey/non-grey
  - opacities
  - convection
- models worse for lower mass stars (cooler, molecules)
- published pre-main-sequence tracks:
  - Swenson, F. J., Faulkner, J., Rogers, F. J., & Iglesias, C. A. 1994, ApJ, 425, 286
  - D'Antona, F. & Mazzitelli, I. 1994, ApJS, 90, 467
  - D'Antona, F., Ventura, P., & Mazzitelli, I. 2000, ApJ, 543, L77
  - Baraffe, I., Chabrier, G., Allard, F., & Hauschildt, P. H. 2002, A&A, 382, 563

Testing PMS Evolutionary Tracks

Spectroscopic, double-lined, eclipsing binaries are able to provide good constraints on a star's position in the H-R diagram

- yield both masses and radii for the stars
- unfortunately, they are very rare
  Casey et al. (1998): Ty Coronae

$$
\begin{aligned}
M_1 &= 3.16 \pm 0.02\, M_\odot \\
L_1 &= 67 \pm 12\, L_\odot \\
T_1 &= 12,000 \pm 500\,\mathrm{K} \\
M_2 &= 1.64 \pm 0.01\, M_\odot \\
L_2 &= 2.4 \pm 0.8\, L_\odot \\
T_2 &= 4900 \pm 400\,\mathrm{K}
\end{aligned}
$$

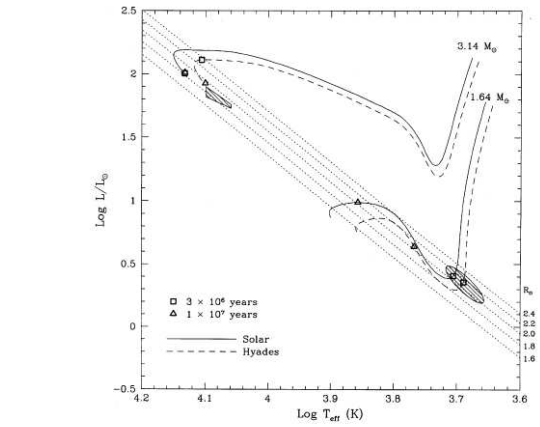

FIG. 8.—Location of TY CrA primary and secondary stars in the theoretical H-R diagram. The hatched regions designate high-confidence domains for the primary and secondary stars based on light-curve analyses (§ 6.2). Dotted lines are drawn at constant radii. Solid and dashed curves correspond to pre–main-sequence tracks of Swenson et al. (1994), calculated for the masses of the primary and secondary of TY CrA. Tracks for solar (*solid curve*) and Hyades (*dashed curve*) compositions are shown. Squares and triangles mark isochrone points at ages of 3 and 10 Myr, respectively.

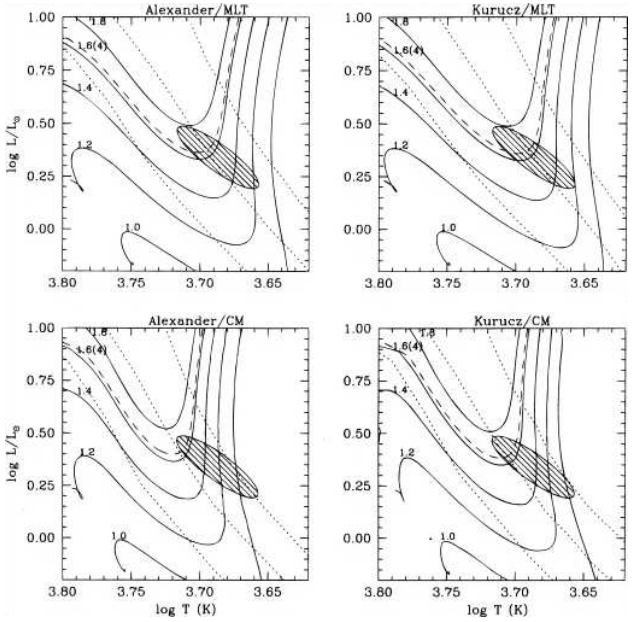

FIG. 13.—Theoretical H-R diagrams centered on the secondary of TY CrA. The solid curves are pre–main-sequence evolutionary tracks from D'Antona & Mazzitelli (1994). The dashed curve corresponds to a 1.64 $M_\odot$ track, derived by interpolating between the 1.6 $M_\odot$ and 1.8 $M_\odot$ tracks. Dotted lines are isochrones drawn at 1, 3, and 10 Myr. The hatched ellipse is the high-confidence domain based on light-curve analyses. The four panels show different combinations of opacities and convection models, as labeled (see § 6.2).

(Casey, B. W., Mathieu, R. D., Vaz, L. P. R., Andersen, J., & Suntzeff, N. B. 1998, AJ, 115, 1617)

Effects of Accretion on PMS Tracks

- see Tout, C. A., Livio, M., & Bonnell, I. A. (1999)
- tracks depend on
  - metallicity
  - accretion history
  - initial state of the star
- an incorrect metallicity can result in errors of
  - a factor of ~ 2 in mass (between $Z = 0.001$ – 0.02)
  - a factor of ~ 10 in age
- for a fixed metallicity
  - accretion history can alter mass estimate by up to 50% (but $\lesssim$ 20% for masses $\lesssim 0.5 M_\odot$)
  - accretion history can alter ages by factors of 2–5

Typical errors in estimating mass due to unknown accretion history

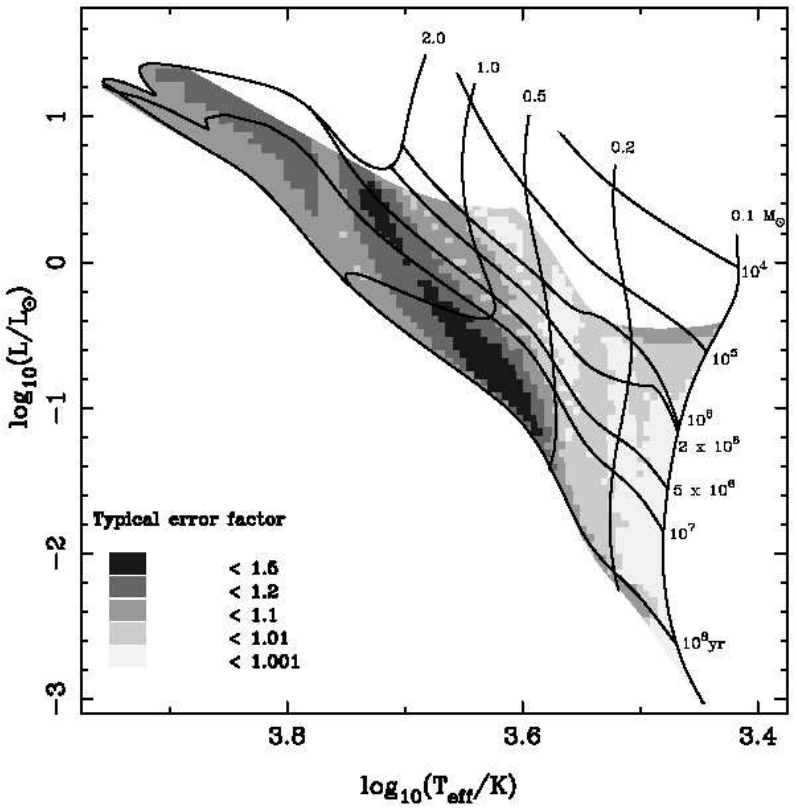

Figure 13. The distribution of the factor by which mass at a given point in the HR diagram differs between our standard accreting tracks and non-accreting tracks. Over most of the diagram the difference is small, being nowhere more than 50 per cent. At temperatures less than about $10^{3.76}$ K the accreting mass is larger, while at higher temperatures the accreting mass is smaller. Some non-accreting tracks and isochrones are overlayed, and the shaded region is that for which we have both accreting and non-accreting tracks available. Twice as many accreting tracks as plotted in Fig. 2 were required to achieve the resolution of this figure.

(Tout, C. A., Livio, M., & Bonnell, I. A. 1999, MNRAS, 310, 360)

Typical errors in estimating age due to unknown accretion history

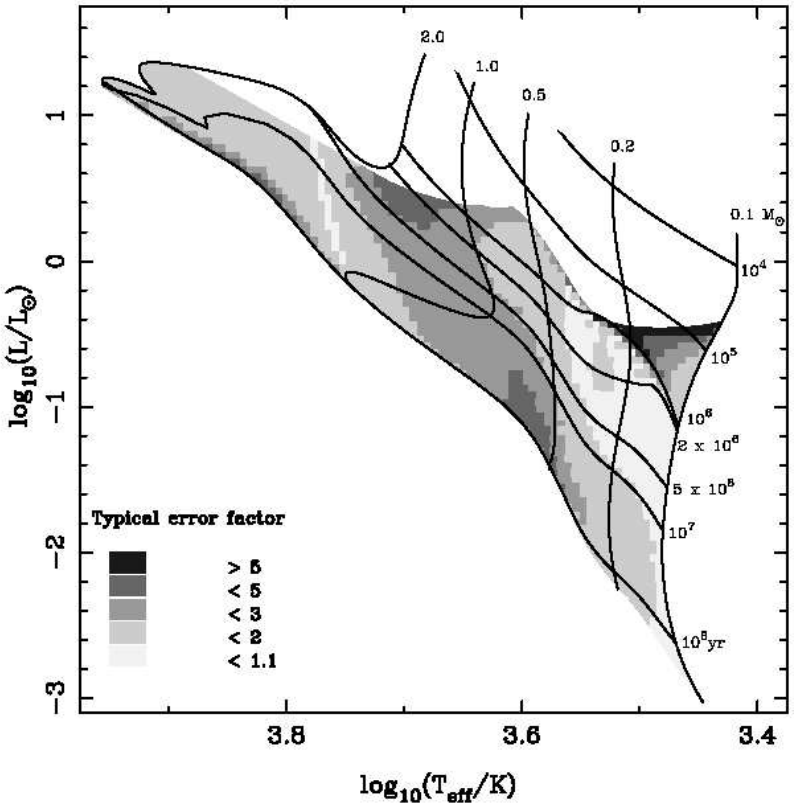

Figure 14. The distribution of the factor by which age at a given point in the HR diagram differs between our standard accreting tracks and non-accreting tracks. For temperatures less than about $10^{3.76}$ K the accreting stars are younger (i.e., they appear older than they are when their age is estimated by comparison with non-accreting tracks), while at higher temperatures they are older. Some non-accreting tracks and isochrones are overlayed, and the shaded region is that for which we have both accreting and non-accreting tracks available. Twice as many accreting tracks as plotted in Fig. 2 were required to achieve the resolution of this figure.

(Tout, C. A., Livio, M., & Bonnell, I. A. 1999, MNRAS, 310, 360)